Plasmonically Amplified Fluorescence Assays for Ultrasensitive Detection of Biomarkers

Master Thesis

Submitted in partial fulfilment of the requirements for the academic degree of

Diplomingenieurin (Dipl.-Ing.in)

Submitted by

SIMONE HAGENEDER

AIT - Austrian Institute of Technology
BOKU - University of Natural Resources and Life Sciences

December 2015

Supervisor: Prof. Dr. Wolfgang Knoll
Department for Nanobiotechnology

Dr. Jakub Dostálek

Acknowledgements

I would like to express my gratitude to Prof. Wolfgang Knoll for his kind offer to supervise my thesis.

My deepest appreciation goes to my group leader Dr. Jakub Dostálek, for his guidance and for giving me the opportunity to start working in his group, and the trust he still shows in me.

Thanks to Dr. Tomáš Riedel and Dr. Martin Bauch for all their help in saliva and sinusoidal grating experiments.

Furthermore I would like to thank Khulan Sergelen for providing expertise in times of need and my special thanks go to Imran Khan, for his support in long working hours. These people I do not only want to call my colleagues, but my very close friends.

I am very thankful to my loved ones, especially my parents, who have supported me throughout my life, letting me do things my own way.

Finally, I would thank the whole Biosensor Technologies Group at AIT for immediately taking me into their group with open arms, all their help on the way and countless coffee breaks.

Statutory Declaration

I declare that I have authored this thesis independently, that I have not used other than the declared sources or resources, and that I have explicitly marked all material which has been quoted either literally or by content from the used sources.

Eidesstattliche Erklärung

Ich erkläre an Eides statt, dass ich die vorliegende Arbeit selbstständig verfasst, andere als die angegebenen Quellen oder Hilfsmittel nicht benutzt, und die den benutzten Quellen wörtlich und inhaltlich entnommene Stellen als solche kenntlich gemacht habe.

_____

Simone Hageneder, December 2015

Abstract

Nowadays fast, cheap and reliable detection is of increasing need in various fields, including early cancer diagnosis and infectious diseases.

This thesis deals with investigating assays for the detection of biomarkers with enhanced fluorescence signal. The plasmonic amplification of fluorescence light emitted by fluorophores used as labels in these assays make it possible to detect even trace amounts of these molecules.

In this regard, the employment of two fluorescence assays on different plasmonic biosensor platforms is shown.

The first sensor design concerns the detection of the sepsis biomarker Interleukin 6 (IL-6) at medically relevant concentrations in serum on nanostructured plasmonic chips.

Secondly, the analysis of Hepatitis B antibodies in clinical serum and saliva samples utilizing a zwitterionic brush architecture with enhanced anti-fouling properties is demonstrated. The obtained results were validated against results from standard ELISA.

The possibility to detect analytes, even in complex biological fluids, at trace amounts can be seen as a basis for future sensor applications.

Kurzfassung

Heutzutage steigt der Bedarf an schneller, günstiger und zuverlässiger Detektion in verschiedensten Bereichen, einschließlich der Krebsfrüherkennung und der Detektion von Infektionskrankheiten.

Diese Diplomarbeit beschäftigt sich mit der Untersuchung von Assays für den Nachweis von Biomarkern mit verbessertem Fluoreszenzsignal. Die Plasmonenverstärkung von Fluoreszenzlicht, welches durch Fluorophore, die als Markierungen in diesen Assays verwendet werden, emittiert wird, machen es möglich, sogar Spuren dieser Moleküle nachzuweisen.

In dieser Arbeit wird die Verwendung von zwei Fluoreszenzassays auf verschiedenen plasmonischen Biosensorplattformen gezeigt.

Das erste Sensordesign betrifft die Detektion des Sepsis-Biomarkers Interleukin 6 (IL-6) in medizinisch relevanten Konzentrationen im Serum auf nanostrukturierten Plasmonenchips.

Zweitens wird die Analyse von Hepatitis B-Antikörpern in klinischen Serum- und Speichelproben unter Verwendung einer zwitterionischen Bürstenarchitektur mit verbesserten Anti-Fouling-Eigenschaften demonstriert. Die erhaltenen Ergebnisse wurden mit Ergebnissen von Standard-ELISA-Tests bestätigt.

Die Möglichkeit, Analyten auch in komplexen biologischen Flüssigkeiten in Spuren nachzuweisen, kann als eine Grundlage für zukünftige Sensoranwendungen gesehen werden.

Table of Contents

TABLE OF CONTENTS

List of Figures and Tables

LIST OF FIGURES

LIST OF FIGURES

List of Abbreviations

Anti-HBs	Hepatitis B surface Antibody
ATR	Attenuated Total Reflection
BRE	Biorecognition Element
ELISA	Enzyme-Linked Immunosorbent Assay
HBsAg	Hepatitis B surface Antigen
IL-6	Interleukin 6
LOD	Limit of Detection
MEF	Metal Enhanced Fluorescence
POCT	Point of Care Testing
RI	Reflective Index
SAM	Self-assembled Monolayer
SP	Surface Plasmon
SPCE	Surface Plasmon Coupled Emission
SPFS	Surface Plasmon Fluorescence Spectroscopy
SPR	Surface Plasmon Resonance

1. Aim and Structure

Ultra-sensitive detection for early diagnosis and more convenient monitoring of diseases are prominent topics of biomedical research. Through the rapid progress made in recent years in the fields of genomics, proteomics and bioinformatics, molecules associated with diseases which can serve as biomarkers are steadily identified.

For the analysis of these biomarkers ELISA (enzyme-linked immunosorbent assay) testing in the laboratory remains the "golden standard". But even nowadays this analysis is often cost- and time consuming and lacks the miniaturization needed for so-called POC (Point-of-Care) applications which allow analysis close to the patient.

This leads to a demand for simple devices capable of fast and reliable detection of clinically relevant analytes. For this purpose surface plasmon resonance (SPR) biosensors were found to hold great potential for point-of-care testing (POCT). A traditional SPR based biosensor on its own may not be a powerful enough tool for certain analytes in POCT, such as small molecules, very dilute samples or in the case of saliva samples. The combination of fluorescence spectroscopy with the well-established SPR spectroscopy in order to enhance the signal obtained in binding events is addressed in this thesis.

Concepts are shown which provide the possibility to rapidly detect biomarkers with the high sensitivity and specificity needed for POCT.

Two different biomarkers serve as model analytes for the assays developed in the course of the experiments: Namely, interleukin 6 (IL-6) and hepatitis B antibodies (anti-HBs). The standard techniques for the detection of these biomarkers are well established. This thesis aims at adapting these principles

into a functional biosensor device. Different approaches of implementation have been developed, always focusing on ultra-sensitive detection.

Firstly a short insight into the physical and biological principles will be given, as well as a deeper explanation of the methods used.

Two different sensor designs are discussed. The first part describes the use of plasmonic relief gold gratings for amplified fluorescence assays (Surface Plasmon-enhanced Fluorescence Spectroscopy – SPFS). The fabrication and the application for an assay detecting IL-6 biomarkers will be shown, as well as the sensing in real samples.

The second part of the thesis will explain the combined usage of an SPR and SPFS system for the detection of anti-HBs in clinical serum and saliva samples utilizing zwitterionic brushes.

2. Background

2.1. Biosensors

While searching for cheap and fast tests, which can be used outside of centralized laboratories, in doctor's offices, in the field, at home or *in vivo*, the first so-called biosensors had been developed. Early successful examples include pregnancy tests or fertility monitors based on immunoassays. In general, as shown in fig.1, a biosensor is defined as a device using a transducer made to convert biological processes into a signal which can be measured (Lowe, 1985).

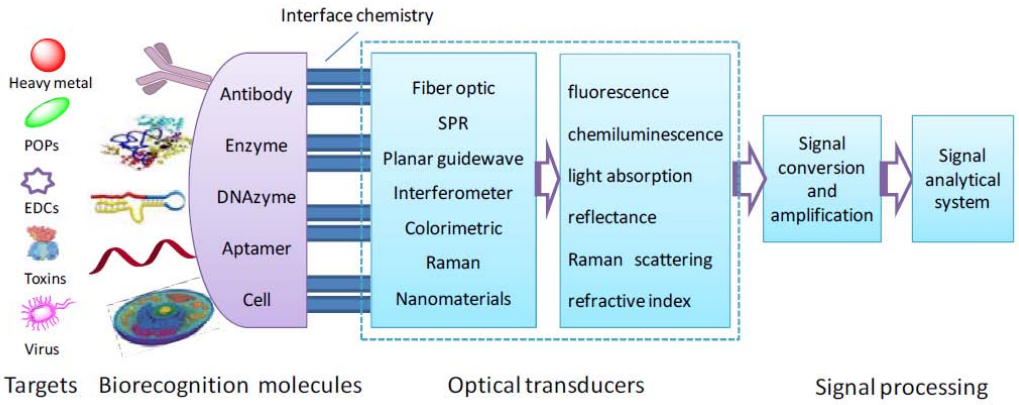

Figure 1: Schematic of a biosensor showing biorecognition, interface and transduction elements (Long et al., 2013).

In the 1980s Liedberg et al. developed the first surface plasmon resonance (SPR)-based biosensor for monitoring of molecular interactions. It was applied for immunoassays, with IgG immobilized on the sensor surface which was probed by confined optical field of resonantly excited surface plasmons (SPs). After injection of anti-IgG into the biosensor, binding was observed as a shift in the SPR, where concentrations as low as 0.2 µg/mL were detectable (Liedberg et al., 1983).

Since the first SPR sensor concept, there have been a considerable amount of applications in different fields. The commercialization of an SPR sensor instrument for immuno-sensing in 1990 by BIAcore has led the way for higher sensitivity and throughput (Homola, 2003),(Biacore, 2015).

As the company name already indicates, the most prominent applications of SPR lie in the field of chemical and biological analysis and the study of bio-molecular interactions (BIA). The advantage to have real time, label-free detection, and at the same time being able to detect very low concentrations, led to many publications in various fields including food safety (Huang et al., 2011), environmentally relevant compounds (Dostálek and Homola, 2006) and, of course, medical diagnostics (Mascini and Tombelli, 2008).

In case of, SPR-based affinity biosensors, the biorecognition elements are attached close to a metal surface, where, upon binding of analyte present in a liquid sample, the change of refractive index (RI) is optically measured.

2.2. Point of Care Diagnostics

Not all diagnostic technologies need cost-intensive highly equipped and staffed infrastructure. Some technologies can be decentralized and provide simplified analysis through automated portable devices. Therefore point-of-care testing (POCT), done at or near the site of patient care, provides fast detection and diagnosis and less effort for the patient. It targets mainly nurses and clinicians, for quick screening of diseases and biomarkers and monitoring of treatment progress (Kost et al., 1999).

As much advantages as this offers, the demands for such a device are higher; such as being inexpensive and robust, giving quick and easy instructions to the user, simple handling (e.g. one-step assays without sample treatment by the user), and showing reliable results. Smartphones could work as interpreters

between the interface and the user, using apps to analyse the measured signal and give immediate response (Wild, 2013).

2.3. Detection of Biomarkers in Different Bodily Fluids

One promising field for the application of biosensors is POC biomarker detection. The term biomarker, short for biological marker, is most commonly defined as "a characteristic that is objectively measured and evaluated as an indicator of normal biological processes, pathogenic processes, or pharmacologic responses to a therapeutic intervention" (National Institute of Health Biomarkers Definitions Working Group) (Gaebel and Zielasek, 2008).

This is a recently introduced term, and from this broad definition a biomarker can be many things e.g. the raise in temperature during fever, blood pressure for the risk of stroke, C-reactive protein (CRP) or IL-6 for inflammation. It can be used for diagnosis, monitoring, prevention and prediction of disease or responses to drugs.

Common clinical diagnosis is mainly done in blood, especially when it comes to detection of biomarkers. But as this has certain disadvantages, research is also focussing on other bodily fluids (e.g. urine, saliva, oral fluid or peritoneal fluid). In the case of saliva, sample collection is non-invasive and simple. This makes saliva diagnostics an excellent means especially for testing in developing countries, having very low demands in terms of collection, storage, shipping and handling, and is considered safer than serum, as persons handling samples are less likely to get in contact with blood-borne diseases (Lee and Wong, 2009).

The first challenge of detection in saliva is, compared to blood, only little is known about its composition. Nevertheless, it is an equally complex fluid as blood which contains a huge variety of enzymes, hormones, antibodies, growth factors and antimicrobial constituents. This includes many biomarkers for diseases as well, but in much lower concentration (Lee and Wong, 2009).

The second challenge is fouling from complex matrices like blood, saliva or urine, a major concern in bioanalytics. Proteins deposit on the surface and change the material's properties, which leads to an interference with the sensor signal in a biosensor, as the signal from fouling can be several orders of magnitude higher than the signal from the sample (Jiang and Cao, 2010).

2.3.1. Interleukin 6

One of the biomarkers used as a model analyte in this thesis is IL-6, which belongs to the family of cytokines and is well-known for its role in regulating inflammatory and immune responses. However, IL-6 has also been found to be involved in a range of other processes inside the body, e.g. IL-6 levels were observed to rise in exercise, working in a hormone-like manner (Fischer, 2006), in neurological diseases like depression, through epigenetic modifications in the brain or regulation of cancer progression (Foran et al., 2010)(Anestakis et al., 2015), just to name a few.

Despite the variety of functions of IL-6, the most prominent role of IL-6 is in sepsis. Infection from pathogens (viruses, fungi, or bacteria) triggers the host's immune response, leading to life-threatening organ malfunction. The estimated annual worldwide incidence rate is around 56-91 cases per 100,000 people and a mortality rate of 30%, with the number still rising (Danai and Martin, 2005)(Jawad et al., 2012).

In the case of sepsis, it is difficult to distinguish from other infectious diseases (Harbarth et al., 2001). The half-life of IL-6 in serum is in the minute-range, demanding for fast and reliable detection e.g. in hospital intensive care. However, if diagnosed early, it can be cured easily with the help of antibiotics.

IL-6 can promote the cell response through binding to two different receptors. Classically, to a high-affinity receptor complex consisting of membrane-bound glycoproteins; IL-6R, an 80kDa low-affinity binding receptor,

and at least one gp130 signal-transducing element which is required for high affinity binding to the complex, but is not binding IL-6 itself. Some processes are also associated with the soluble form of the receptor, sIL-6R, which forms a complex with IL-6, binding to the gp130 glycoprotein (Jones, 2005).

IL-6 levels in serum can range widely, from <1-10 pg/mL in healthy individuals (Knudsen et al., 2008), to higher than 1000 pg/mL during sepsis (Jekarl et al., 2013) (Harbarth et al., 2001).

The standard technique of detection is ELISA in blood, of which results often need several days to reach the patient. State-of-the-art diagnostic tools show a LOD of 1.5 pg/mL (Roche GmbH, 2015), but they require specialized laboratory infrastructure, whereas commercial POC devices typically show a minimum LOD of 50 pg/mL (Milena Biotec, 2015).

2.3.2. Hepatitis B antibodies

Hepatitis B is a disease of the liver, caused by the hepatitis B virus (HBV), which has an incidence rate of around 350 million people around the world. Around 10% of all virus-carriers develop chronic hepatitis (strongly depending on age). Approximately 20-25% of these chronically ill patients additionally develop progressive liver disease which can lead to cirrhosis.

Therapy of Hepatitis B is very difficult and expensive which makes vaccination the most important tool in order to stop spreading and decrease the number of infections (Great Britain Department of Health and Joint Committee on Vaccination and Immunisation, 2006). Active vaccination exists since 1981 and consists of purified hepatitis B surface antigen (HBsAg) (Blumberg, 1977). A three dose series usually provides efficient protection in the form of antibodies against the hepatitis B surface antigen (anti-HBs), but the actual time of protection provided is not known (Poorolajal et al., 2010). Therefore, the level of anti-HBs after vaccination or recovery from disease has to be checked regularly, especially for elevated risk groups, thus making them a very potent biomarker

(Gitlin, 1997). According to WHO, a titer >10 mIU/mL is considered protective against HBV infection (Mahoney, 1999).

Similar to IL-6, results of an HBV test are routinely obtained by a standard ELISA immunoassay in laboratories which usually require certain infrastructure, trained personnel and take up to several days to yield results. Especially the risk of false positives is generally very high (Huzly et al., 2008).

2.4. Surface Plasmon Resonance Biosensors

Surface plasmons (SPs) are collective fluctuations of the electron density at the metal-dielectric interface.

Otto (Otto, 1968)*, Kretschmann* and *Raether* (Kretschmann, E and Raether, H., 1968) were the first ones in the late 1960s to show the optical excitation of SPs, called Attenuated Total Reflection (ATR) method, utilizing prisms. Two different prism coupling geometries are known, shown in fig. 2: The one most widely used in biosensing is the *Kretschmann* configuration (fig.2a), which consists of a high reflective index (RI) prism with a thin metal layer. The light is going through the prism and is reflected at its base, generating an evanescent wave which can be coupled with an SP at the outer metal surface. The second one is the *Otto* configuration (fig. 2b), where a small gap is separating the prism and the metal. It is used for thicker metal films and when it is not desirable to have direct contact with the metal surface (e.g. studies of the surface quality), due to the difficulty to control the gap between the two interfaces.

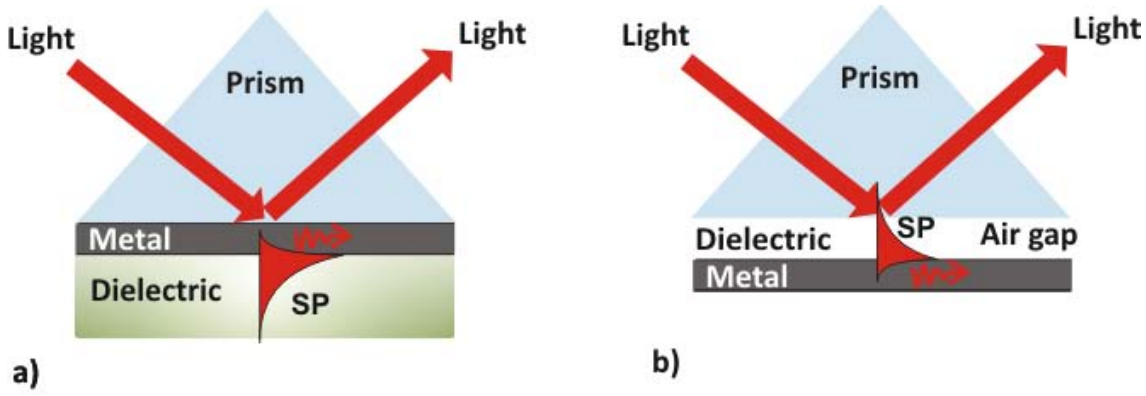

Figure 2: Different kinds of configurations using ATR for prism coupling in a) Kretschmann and b) Otto configuration.

As depicted in fig. 3, analytes are binding to the metal surface with biorecognition elements (BRE, see section 2.5.4) attached, the RI at the prism side is not changing, but the RI near the metal surface is increasing. This leads also to a change in the propagation constant and alters the coupling conditions between light and SPs, which is then to be detected. Due to these changes in resonance conditions, the characteristics of the light wave are altered (Boozer et al., 2006)(Liedberg et al., 1983).

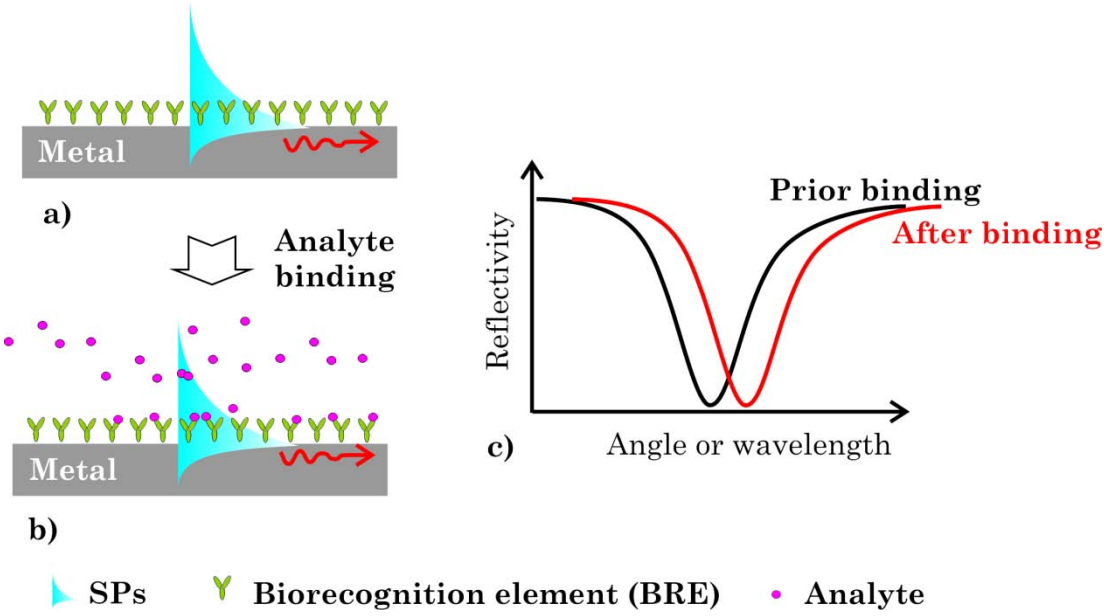

Figure 3: Principal scheme of an SPR biosensor: a) BRE bound to the metallic surface b) analytes in a liquid sample binding to the BRE. c) RI change due to binding of analyte leads to a change in SPR signal.

In an SPR sensor with angular modulation these processes lead to a shift in resonance angle, in sensors with wavelength modulation the shift of the wavelength or in a change of light intensity in case of intensity modulation, just to name the most important modalities of SPR biosensors (fig. 3c).

Therefore an SPR sensor is a very good means to measure binding events in real-time through monitoring the shift due to the change in RI in the vicinity to the surface (fig. 3c).

These real-time measurements are useful for tracking the kinetics of molecular interactions. This can be implemented through monitoring the shift of the angle at the resonance angle or wavelength at the dip. A typical response is shown in fig. 4, in a so-called sensogram.

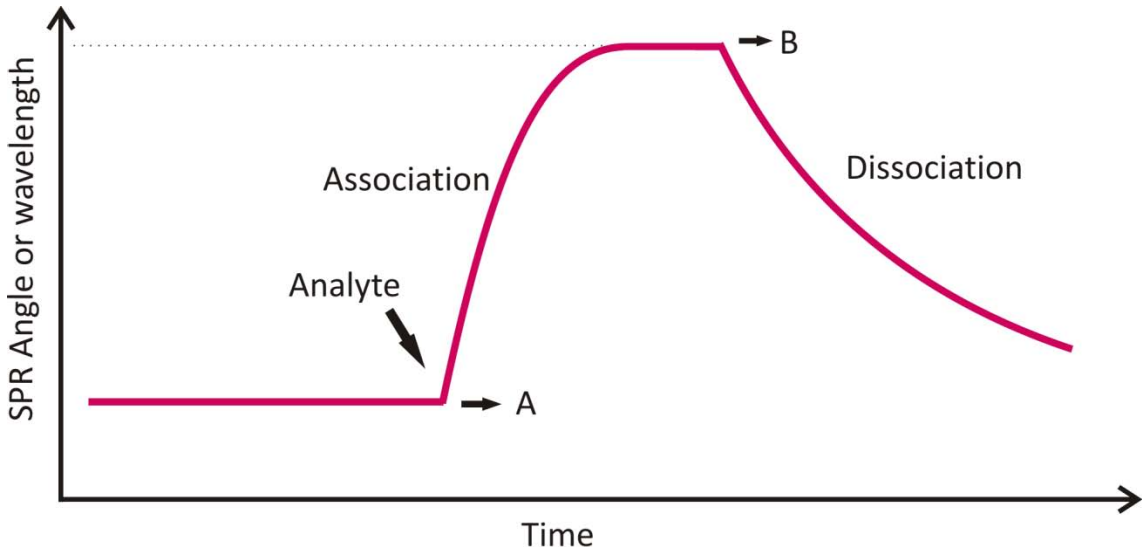

Figure 4: Schematic of a sensogram: Real time analysis of the binding after injection (arrow) of the analyte. The shift of the resonance angle or wavelength (A to B) is due to the increase associated with the binding of analyte to the surface.

In a common experiment, firstly the buffer baseline of the response is established. The association phase upon injection of the analyte (A) and specific binding is indicated by the gradual increase in signal until saturation is reached. At time point B, the sensor is rinsed with buffer and the dissociation phase starts.

For most sensing purposes the SPR sensor consists of a glass substrate coated with a thin metal film that is optically matched to a prism in the Kretschmann configuration. Gold films are the first choice when it comes to SPR detection, mainly because they are very stable and do not tarnish (Szunerits et al., 2008).

An alternative method for using light to achieve SP excitation without prisms is grating coupling, seen in fig. 5.

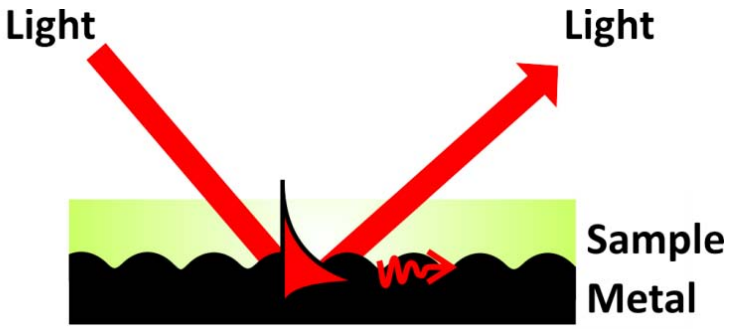

Figure 5: Excitation using grating coupling

For periodically corrugated metallic surfaces are used, diffraction allows to phase-match an incident wave with SPs. The first grating coupling based biosensor was developed by Cullen et al. in the 1980s (Cullen et al., 1987). They have been used less frequently in SPR biosensing, but unlike prism couplers, there is no need for the exact control of the thickness of the metal layers and they can also be fabricated into plastic substrates, enabling cheap mass production (Liley, 2002).

Sinusoidal gratings are best suited for grating coupling; the resonant wavelength of the grating structure is determined by the period and the amplitude of the grating. The angle of light coupling changes with the binding of the biomolecules on the surface.

The grating structure is illuminated at varying incidence angles and the differences in the reflected light intensity can be detected, thereby measuring binding curves in real-time.

2.5. Fluorescence

Fluorescence describes the phenomenon of the ability of molecules, called fluorophores, to be excited and emitting energy in the form of light (Lakowicz, 2006).

A most common schematic, Jablonski diagram, explains the processes going on between the adsorption and emission of light during fluorescence and is

presented in fig.6 below. It shows the transitions of the fluorophore from the ground state (S_0) to an excited state (S_1) by absorption of a photon. The fluorophores can exist in different vibrational energy levels inside one electronic energy level. Immediately after, internal conversion occurs and the fluorophore relaxes to the lowest vibrational level of S_1 state. After that, transition to the ground state (S_0) occurs, accomplished by emitting a photon.

The emission occurs at higher wavelengths (less energy) than the absorption, which is referred to as the Stoke's shift.

An important characteristic of a fluorophore is its quantum yield. It defines the number of photons emitted per photon absorbed. The higher the quantum yield, the brighter the emitted light.

Fluorescent quenching comprises all processes where fluorescence intensity is decreased. This can happen if the fluorophore collides with another molecule, forms a non-fluorescent complex with another molecule or simply by attenuation of the incident light through the fluorophore or an absorbing species (Lakowicz, 2006).

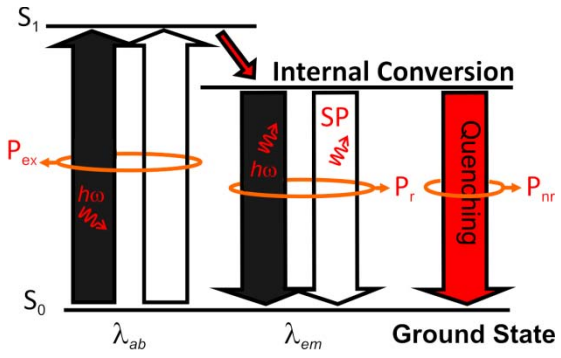

Figure 6: Jablonski diagram highlighting the transitions of free fluorophores (black and red) and interaction of fluorophores with the metal (white).

Far from saturation, the fluorescence emission P_{em} is dependent on the excitation rate P_{ex}, the radioactive decay rate P_r and the non-radiative decay rate P_{nr}. (see fig. 6) (Dostálek and Knoll, 2008):

$$P_{em} \propto P_{ex} \frac{P_r}{P_r + P_{nr}} \quad (1)$$

A fluorophore can be used as a label e.g. of an antibody or other biomolecule which is specific for the analyte of interest. Fluorescence is widely used, especially in biological sciences and medical diagnostics, but also exploited by various other fields, as it is highly sensitive.

In order to further enhance the signal in fluorescence assays, fluorophores can couple with SPs. The fluorophores can use the enhanced field intensity of SPs on metals. This interaction is the basis of plasmon-enhanced fluorescence (PEF) or metal-enhanced fluorescence (MEF).

An interplay of three mechanisms exist that makes it possible to enhance the emitted fluorescence intensity through changing the behaviour of the fluorophore.

- Increase of fluorophore excitation rate P_{ex} (rate of excitation from ground state to excited state) leading to higher fluorescence emission
- Improve fluorophore quantum yield
- Increase in directivity of emission (collect and re-emit light in certain directions)

2.5.1. Surface Plasmon Coupled Emission

Various studies in the 1970s reported that fluorophores placed on a metallic surface had a much reduced lifetime due to coupling with surface lossy waves (quenching due to dipole-dipole interactions) and SPs (Weber and Eagen, 1979)(Drexhage, 1970). This occurs strongly if the fluorophore is put close to the metal (<10-20 nm, short dye-to-metal distances) (Yu et al., 2004).

Surface plasmon-coupled emission (SPCE) is a result of the near-field interaction of a radiating molecule with a layered structure containing a thin metal film. On the metallic layer molecules close to the interface emit light via SPs that are subsequently re-emitted in a very narrow angular range.

SPCE can be seen as inversely related to SPR (Lakowicz, 2004)(Gryczynski et al., 2004) and it is observed at λ_{em}. It provides a means to efficiently collect fluorescence light and suppress background signals.

2.5.2. Surface Plasmon Enhanced Fluorescence Spectroscopy

Fluorophores in close proximity to a metal surface can be coupled with the strong electromagnetic field of SPs at λ_{ex}. This can lead to an increase in the excitation rate (Lakowicz, 2005). This system has either been used with the Kretschmann configuration (ATR) or diffraction on periodically corrugated metallic surfaces for coupling of the plasmons and is referred to as Surface Plasmon Enhanced Fluorescence Spectroscopy (SPFS) (Liebermann and Knoll, 2000), (Neumann et al., 2002).

By 1999 the first concept of a SPFS biosensor was presented, combining traditional SPR biosensing with SPFS (Liebermann and Knoll, 2000).

The fluorescence enhancement provided by SPFS allows for a highly increased sensitivity and therefore a decrease in the LOD (Limit of detection) and the ability to detect even trace amounts of analyte (Toma et al., 2015). Another very important advantage is that not only is it possible to monitor the fluorescence signal, but also SPR measurements can be deduced simultaneously (Ekgasit et al., 2005).

2.5.3. Surface architectures

The surface architecture of a biosensor should be highly specific and non-specific adsorption should be avoided. This is especially challenging when it comes to the quantification of molecules like biomarkers in complex matrices such as urine, serum or saliva. We witnessed rapid advances in non-fouling or anti-fouling surfaces, which can be used to coat the metal surface before the immobilization of BREs. Some common approaches are outlined below.

Self-assembled monolayers

In SPR –based biosensor applications, self-assembled monolayers (SAMs) are widely-used to design the properties of the metal interface. Self-assembly occurs widely in nature and can be generally described as the use of simple building blocks to spontaneously form complex but ordered structures (Schreiber, 2000). The simplest example would be lipid bilayers which membranes are formed of. In the laboratory, monolayers are formed by adsorption of e.g. alkanethiols or disulfides on metal surfaces (Knoll et al., 1997). If the chains have sufficient length, they form a densely packed layer oriented normal to the metal surface. Thiols with PEG-ending groups provide a very good anti-fouling surface. Studies suggested this to be due to a hydration layer, where water is tightly bound to the SAM via hydrogen bonds. This layer forms physical and energetic barrier to prevent protein adsorption near the surface (Chen et al., 2000)(Herrwerth et al., 2003). In order to provide specific functionality, mixed thiol SAMs in varying ratios are applied (Wild, 2013). Prominent functional end groups like carboxylic groups can be utilized for covalent coupling (see section 2.5.4), biotin end groups can bind streptavidin and subsequently various biotinylated compounds (Löfås and Mcwhirter, 2006) (Busse et al., 2002). Various publications deal with the optimal ratios and alkyl chain lengths to, on the one side, not sterically hinder the binding, and on the other, being able to provide enough and active binding partners for further modifications (Spinke et al., 1993)(Vericat et al., 2010)(Love et al., 2005).

Aside from single chain monothiols, also dithiols are used. They provide a more stable layer and the SAM is assembled faster compared to monothiol SAMs (Subramanian et al., 2006).

Zwitterionic brushes

When handling complex media like serum or saliva, the short hydrophilic chains introduced by SAM surface may not be able to provide enough resistance to fouling (Rodriguez-Emmenegger et al., 2012).

The sort of materials which has shown to suppress fouling to a huge extent are zwitterionic brushes with positively and negatively charged moieties. They are grown by polymerization processes like surface-initiated atom transfer radical polymerization (SI-ATRP) (Blaszykowski et al., 2012). Compared to short chain hydrophilic SAMs their enhanced anti-fouling ability is due to the enhanced surface hydration layer which derives not only from hydrogen bonding, but from stronger ionic solvation by the zwitterionic materials (Chen et al., 2006).

2.5.4. Immobilization techniques

Biorecognition elements

A biorecognition element (BRE) is a functional unit that specifically captures the analyte to be detected. It can be any biomolecule, most widely used are proteins (in particular antibodies). Their usage in bioassays has been first reported in the 1950s, measuring insulin in a radioimmunoassay in unextracted human plasma (Nobel prize in 1977)(Yalow and Berson, 1959).

Earlier, BREs were directly derived from living organisms, but nowadays also synthesized aptamers or imprinted polymers are used (Löfås and Mcwhirter, 2006)(Chambers et al., 2008).

As SPR biosensors can employ a huge variety of BREs, they have to be chosen carefully, taking into account the required specificity (single or multiple analyte detection), operation mode (continuous monitoring or rapid detection of the analyte), and last but not least also the conditions for storage and stability (Dostálek et al., 2006).

Covalent binding

The simplest case for immobilizing molecules acting as BREs on the surface would be the direct adsorption to the metal, which would lead to low coverage, high non-specific adsorption and less bioactive molecules on the surface (Homola et al., 1999). As shortly discussed in section 2.5.3 above, surfaces can be coated with various anti-fouling materials where the BRE can be selectively attached through differently designed coupling chemistries.

Molecules have been shown to covalently bind to the surface using free functional side groups of amino acids, such as amine groups in lysine or thiol groups in cysteine. The molecules to be immobilized are then reacted with following activated moieties:

- amines (lysine, α-amino groups),
- phenols (tyrosine),
- carboxylic acid (aspartic acid, glutamic acid),
- thiols (cystin, cysteine, methionine) or
- other side groups (Arginine, Histidine, Tryptophan) (Brinkley, 1992)

For the coupling of proteins onto SAMs, carboxylic acid moieties are most commonly used, using active esters for their activation and reacting with amine groups on proteins.

Amine coupling

The activation of carboxylic acids with active esters almost always leads to unstable intermediates in water. So it is necessary to find a way to prevent hydrolysis and at the same time make the amine group on the protein as reactive as possible towards the activated carboxylic group. Common and frequently used substances which are also water-soluble are EDC [N-1-Ethyl-3-(3-dimethylaminopropyl) carbodiimide hydrochloride] and CMC {1-cyclo-hexyl-3-[2-(4-methylmopholin-4-yl)ethyl]carbodiimide p-toluenesulfonate)}. In this mechanism, a carbodiimide reacts with a carboxylic acid and forms O-acylisourea. But as the amine is most reactive at a pH 9-10, and the reaction above is optimized at pH 5-6, it may not always be the optimal choice (Wild, 2013).

A second method would be the incorporation of a second chemical, NHS (N-hydroxysuccinimide). The isourea is first made to react separately into a succinimide ester before it is put in contact with the amine to perform the incorporation step (Wild, 2013). Any remaining active carboxylic groups are blocked by injection of high concentrations of ethanolamine.

2.5.5. Assay design

SPR-based biosensors were developed based on both, direct and indirect assay formats.

For a direct assay, the analyte is detected directly through the change in mass on the surface that alters the RI. For small molecules the change of RI may not be enough and it may be necessary to use indirect detection. It requires an additional reaction and sandwich, competitive or inhibition assay formats can be implemented (Stratis-Cullum and Sumner, 2010) (Homola et al., 1999).

In a sandwich assay, an immobilized BRE binds the analyte, which is then detected by a reaction of an additional molecule recognizing another epitope of the analyte. Washing steps are performed between each step.

In fig. 7, the principles for immunoassays, which rely on antibody-antigen recognition, are shown. Immunoassays are widely used since the ELISA technique was developed in the 1970s (Engvall and Perlmann, 1971) (Van Weemen and Schuurs, 1971).

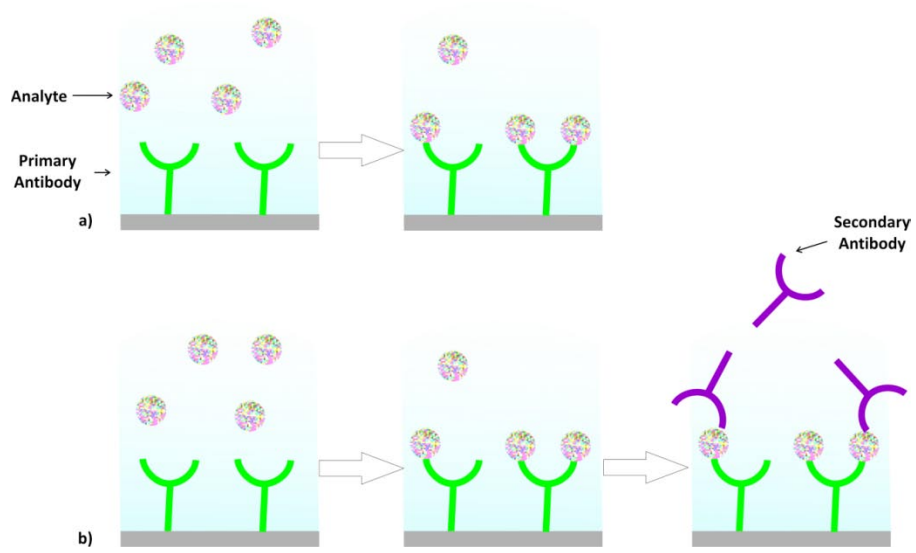

Figure 7: Typically used assay formats in an SPR biosensor: a) direct and b) sandwich assay

Biotin/Streptavidin coupling chemistry

The streptavidin/avidin-biotin binding is one of the strongest interactions; therefore it is in many cases the preferred method for coupling of biomolecules. Biotin is a vitamin which is water-soluble and has a relatively small molecular weight of 244 kDa. The affinity of avidin (or streptavidin) for biotin is around $K_d = 10^{-15}$ M (Wilchek and Bayer, 1998). The introduction of a biotin group to a protein is rather simple. Many commercial kits are available for chemical or

enzymatic biotinylation (eg. Biotin-NHS) and biotinylated proteins can also be purchased (Wild, 2013).

Avidin is a protein found in the egg-white of different animals, i.e. making 0.05 % of total proteins in a chicken egg white. Streptavidin, which itself is around 60 kDa, is the bacterial form of avidin. The difference lies in the isoelectric point, which is rather neutral (avidin around pH 10)(Narain and Sunasee, 2014). Additionally streptavidin does not contain any carbohydrate moieties, making it less prone to non-specific binding and therefore more suitable for bioassays (Gitlin et al., 1990)(Kresge et al., 2004).

As illustrated in fig. 8, streptavidin/avidin hosts four binding sites, and biotin binding does not lower the biological activity of the protein. In a classical assay format, the biotinylated protein bound to the BRE is then detected by a streptavidin/avidin conjugate (e.g. fluorescent dyes or HRP).

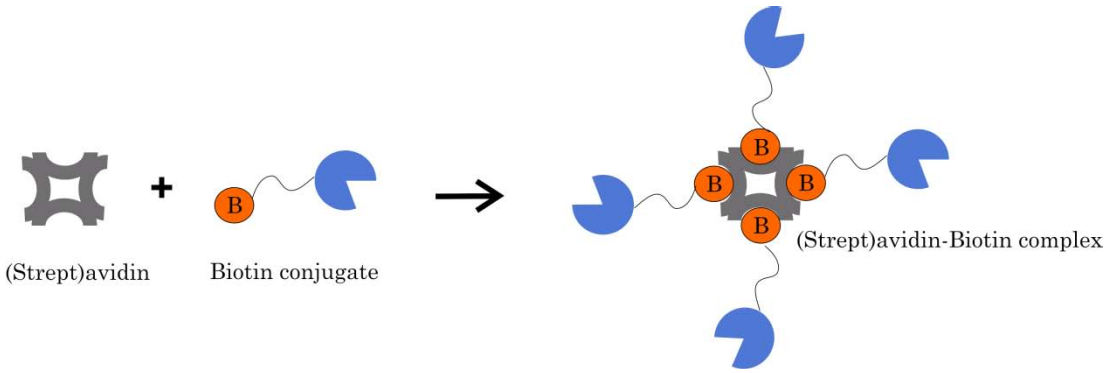

Figure 8: Schematic of the interaction of biotin and (strept)avidin. Four biotin molecules binding to one (strept)avidin.

In order to enhance the signal of the assay, more than one biotin molecule can be attached to a protein, as well as using multiple streptavidin/avidin conjugates (Thermo Fisher Scientific Inc., 2009).

3. Materials & Methods

3.1. Materials

3.1.1. Materials for IL-6 experiments

The carboxylate (SPT 0014A6) and PEG-dithiols (SPT 0013) were purchased from SensoPath Technologies (Bozeman, Montana, US).

EDC [(1-Ethyl-3-(3-dimethylaminopropyl) carbodiimide; cat.No. 22981] and NHS (N-hydroxysuccinimide, cat.No. 24500) were obtained from Thermo Scientific, Waltham, MA, US. Ethanolamine (1M in water) from Sigma Aldrich (St.Louis, MO, US), pH adjusted to 8.5. 10 mM acetate buffer (ACT) with pH 4 was prepared from sodium acetate and acetic acid and the pH was adjusted by HCl and NaOH.

The capture antibody (anti-Human IL-6 purified) against human interleukin 6 (Clone MQ2-13A5; product number 14-7069-85), affinity-purified recombinant protein carrier-free human IL-6 (product number 34-8069) and as a secondary antibody anti-human IL-6 biotin (Clone MQ2-39C3; product number 13-7068-85,) was used, all obtained from eBioscience. Streptavidin Alexa Fluor 647 conjugate in PBS was purchased from Life Technologies, CA, US (product number S32357; in average 3 fluorophores per molecule).

Samples were prepared in PBS pH 7.4 (Phosphate buffered saline, Calbiochem, CA, US, product number 524650-1EA) containing 0.05 % Tween-20 (P9416, Sigma Aldrich (St. Louis, MO, US)) and 1 mg/mL biotin-free Albumin Fraction V (from Roth).

Positive photoresist Microposit S1805 was purchased from Shipley and its developer AZ 303 was acquired from MicroChemicals. Polydimethylsiloxane

elastomer (PDMS) Sylgard 184 was obtained from Dow Corning and the UV-curable polymer Amonil MMS 10 was from AMO GmbH.

3.1.2. Materials for saliva experiments

HBsAg (antigen) (recombinant, adw subtype Cat.# 8HS7-2ad) was obtained from Hytest (Turku, Finland), as well as the antibodies against the antigen [Monoclonal mouse anti-hepatitis B virus surface antigen (anti-HBsAg) Cat.# 3HB12 MAb Hs 41]. Reagents for amine coupling were purchased from Biacore (Amine coupling kit; order number BR-1000-50)

Detection antibodies against monoclonal mouse antibody [Alexa Fluor® 647 Goat Anti-Mouse IgG (H+L) (cat. No. A-21235)] and against human antibodies in the clinical samples [Alexa Fluor® 647 Goat Anti-Human IgG (H+L) (cat. No. A-21445)] were purchased from Molecular Probes (Eugene, OR, US). The Alexa Fluor 647 dye has an excitation wavelength of λ_{ex}=650 nm and an emission wavelength of λ_{em}=668 nm.

The buffers used were phosphate buffered saline (PBS, pH 7.4, Calbiochem, CA, US); HEPES buffer (10mM, pH 7.5); sodium acetate buffer (SA, 10mM, pH 5); Glycine-HCl buffer (20mM, pH 1.5).

The chips modified with zwitterionic brush architecture including the monomers 3-methacryloylaminopropyl-2-carboxyethyl-dimethylammonium betaine (carboxybetaine methacrylamide, CBMAA) and N-(2-hydroxypropyl)methacrylamide (HPMA) were synthesized at the Institute of Macromolecular Chemistry, AS CR, v.v.i., Prague, Czech Republic (Rodriguez-Emmenegger et al., 2012) (Rodriguez-Emmenegger et al., 2011a)(Ulbrich et al., 2000).

Sample collection

The human serum and saliva samples were taken from healthy volunteers from the AIT staff and had been pretested in a certified lab by a reference ELISA method.

The serum samples were taken by incubation of blood in Vacuette 9 ml Z Serum Clot Activator (Greiner Bio One, Frickenhausen, Germany) for 30 min, then centrifuged for 10 minutes at 1,800 g at room temperature.

The saliva samples were obtained from the same donors; they hadn't eaten or drank for 30 minutes prior to the sample taking. The samples were centrifuged for 5 minutes at 16,000 g and the supernatant was aliquoted. Serum and saliva aliquots were stored at -80°C.

3.2. Methods

3.2.1. Optical setups

Setup configurations to be discussed use an identical light source, flowcell and module to collect and deliver fluorescence light to a detector.

Prism coupled SPR sensor

The setup is assembled by the colleagues at the AIT. A He-Ne laser is used for the excitation of SPs (1.5 μW, λ_{ex}= 632.8 nm). It passes through a laser band-pass filter (FL632.8-10 from Thorlabs), a polarizer, and a neutral density filter (1 %). The beam is coupled to a 90 degree prism coupler made of LASFN9 glass, which is optically matched to a disposable sensor chip using immersion oil (Cargille Inc., USA).

The sensor chip is clamped onto a flow cell made from fused silica and contains in- and outlet ports that are connected to the tubings to the attached peristatic pump.

The emitted fluorescence light at λ_{em}=670 nm is collected by a module with a lens (focal length f=50 mm and numerical aperture of NA=0.2, LB1471 from Thorlabs for the IL-6 experiments; length f=35 mm and numerical aperture of NA=0.3 for the anti-HBs experiments), going through a notch filter (XNF-632.8-25.0M from CVI Melles Griot) to block the excitation wavelength λ_{ex} and two bandpass filters (FB670-10 from Thorlabs and 670FS10-25 from Andover Corporation Optical Filter) with the transmission window centered at the λ=670 nm and spectral width of about 10 nm. The fluorescence beam was then focused at the input of a photomultiplier (H6240-01, Hamamatsu) that was connected to a counter (53131A from Agilent). The reflected beam is then detected by photodetector, going to a lock-in amplifier (EG&G Instruments).

The output from the counter was recorded counts per second (cps), the output from the photomultiplier in % light intensity, by using software WasPlas developed at Max Planck Institute for Polymer Research in Mainz (Germany).

Epifluorescence reader

The term epifluorescence derives from fluorescence microscopy, meaning that that light source is placed above (epi) the sensor, and the emitted fluorescence is imaged to the detector by the same objective lens as for the excitation. Devices based on this geometry include fluorescence micro-arrays or, as mentioned, microscopes.

Different to the setup before, the excitation beam is reflected by a dichroic mirror (XF2087 660DRLP from Omega Optical), hits the sensor surface (with the same flowcell clamped on top). The laser intensity was set to 1.5 μW using neutral density filters. The dichroic mirror is tilted by 45 deg where it is highly reflective at the wavelength λ_{ex}=633 nm and transparent at the emission wavelength of λ_{em}=670 nm. The emitted fluorescence passes through the dichroic mirror, a spatial filter that blocks the partially reflected excitation beam at the wavelength λ_{ex}. It is finally collected by the lens and detected.

Multichannel SPR sensor

For measurements done in Prague, a 4-channel SPR biosensor system with ATR Kretschmann configuration was used. Any changes in the reflected SPR wavelength through RI variations are analysed by a spectrometer, separately for each of the four channels. This was developed at the IPE Prague [see (Homola et al., 2005)].

3.2.2. Preparation of sensor chips

The crossed grating structures were prepared by laser interference lithography and replicated via UV nanoimprint lithography (Bauch et al., 2014).

Laser interference lithography

This technique uses two coherent laser beams which interfere, leaving a structure (interference pattern) at the point where they meet, an area of layers of photoresist. It is a technique suitable for structuring of large area and providing a substrate with fine and regular patterned array (van Wolferen and Abelmann, 2011).

UV nanoimprint lithography

Here, as it is depicted in fig. 9, a PDMS stamp was prepared by heat-curing the elastomer (Sylgard 184) over a LIL produced structure master.

The stamp is then released from the master and used for imprinting into a substrate. A UV-photocrosslinkable photoresist is spin-coated on a clean BK7 glass, the PDMS stamp placed over it, and UV-cured at 365 nm (UV lamp Bio-Link 365, Vilber Lourmat) and the stamp is removed. Subsequently the sample can be further processed (in this case: metal deposition).

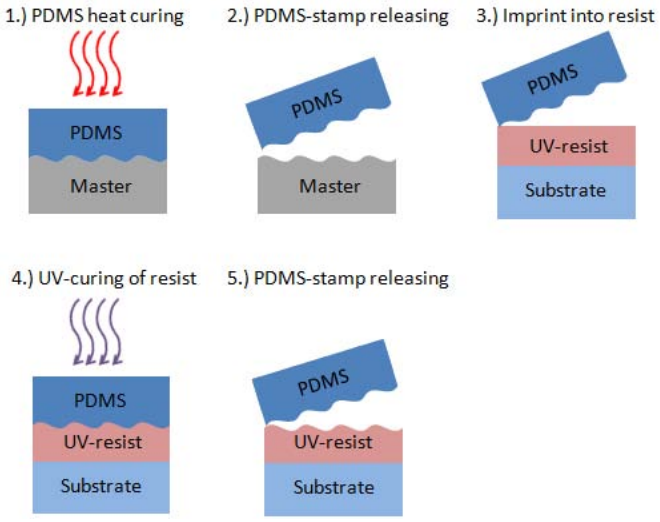

Figure 9: Schematic of UV nanoimprint lithography [Reprinted with permission from (Bauch, 2014)].

Gold layer deposition

On a clean BK7 substrate (or the grating structure already prepared, see section above), metal is deposited using vacuum thermal evaporation (HHV AUTO 306 from HHV LTD). It is a method of thin film deposition, using vacuum to coat objects with pure materials in the nm to μm range. A thicker gold (Au) layer is used to support the plasmon modes, with a thin underlying adhesion layer of Chromium (Cr) or Titanium (Ti) that prevents the delamination of the Au film.

Preparation of SAMs

SAMs were formed overnight on the Au layer, directly after deposition, by incubating in 1 mM ethanolic solution of dithiols mixture.

Preparation of zwitterionic brushes

The two modifications used in the following experiments were copolymerized poly(carboxybetaine acrylamide) [poly(CBAA)] and poly[N-(2-hydroxypropyl) methacrylamide] [poly(HPMA)] brushes (Rodriguez-Emmenegger et al., 2011b)(Rodriguez-Emmenegger et al., 2011a). The architecture of the brush is

depicted in fig. 10. The activation protocol is able to only target one of the polymers (CBMAA) which was put into the polymerisation mixture in a smaller ratio.

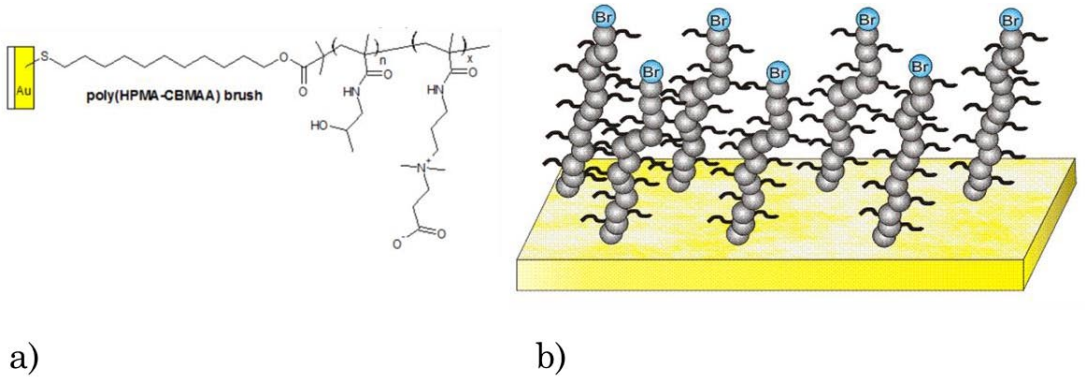

Figure 10: Polymer brush architecture (picture with permission from Tomáš Riedel)

All of these surface modifications were done by the Institute of Macromolecular Chemistry, AS CR, v.v.i., Prague, Czech Republic.

4. Results & Discussion

This thesis presents two collaborative projects. Firstly, an IL-6 sandwich immunoassay was developed and employed for the comparison of two commonly used fluorescence readout geometries with plasmonic amplification of the signal – Chapter 4.1. The epifluorescence (EPF) configuration was investigated with a chip carrying a metallic crossed relief grating that allows for diffraction excitation and out-coupling of surface plasmons. Its performance is compared to the total internal reflection fluorescence (TIRF) method where surface plasmons are generated by using Kretschmann geometry.

In the second project presented in Chapter 4.2, analysis of biomarkers in saliva and serum is investigated by using plasmonic biosensors. As a model system, antibodies against hepatitis B are analysed in these matrices by using surface plasmon resonance (SPR) and surface plasmon-enhanced fluorescence (SPFS) biosensors. In order to cope with strong unspecific interaction of these complex matrices with the sensor surface, novel antifouling polymer brush architecture is used at the interface.

The first project was pursued in collaboration with Dr. Martin Bauch at the AIT in Vienna. Dr. Bauch prepared grating master structures and developed the optical instrument used in the experiments. The author functionalized the investigated chips, carried out assay experiments and evaluated the measured data.

The second project was a joint collaboration with Dr. Tomáš Riedel, Institute of Macromolecular Chemistry, Prague, Czech Republic. Dr. Riedel and his colleagues prepared zwitterionic brush structures and analysed serum and samples by surface plasmon resonance in Prague. The author in collaboration

with Dr. Riedel employed surface plasmon-enhanced fluorescence for the analysis of saliva samples at AIT in Vienna.

4.1. Plasmonically amplified IL-6 assay: total internal reflection vs epifluorescence readout

As shown in fig. 11, *in situ* optical readout of fluorescence assay was carried out by using identical optical components arranged in EPF and TIRF geometry. The fluorescence signal was detected via a transparent flow cell. The sensor surface was probed by resonantly excited SPs in both implementations in order to amplify the output signal. In the EPF method, the diffraction allowed to enhance the excitation rate of fluorophore at the surface by excitation of SPs at λ_{ex}. In addition, it simultaneously exploited the directional diffraction out-coupling of fluorescence emitted via SPs at λ_{em} which is then delivered to the detector [investigated in a previous work (Bauch et al., 2014)]. In the TIRF configuration, fluorophores are excited at the λ_{ex} by SPs utilising prism coupling and the Kretschmann configuration (see section 2.4.). At the emission wavelength λ_{em}, the majority of fluorescence light is emitted via surface plasmons that are re-emitted across a thin metal film into the prism due to reverse Kretschmann coupling.

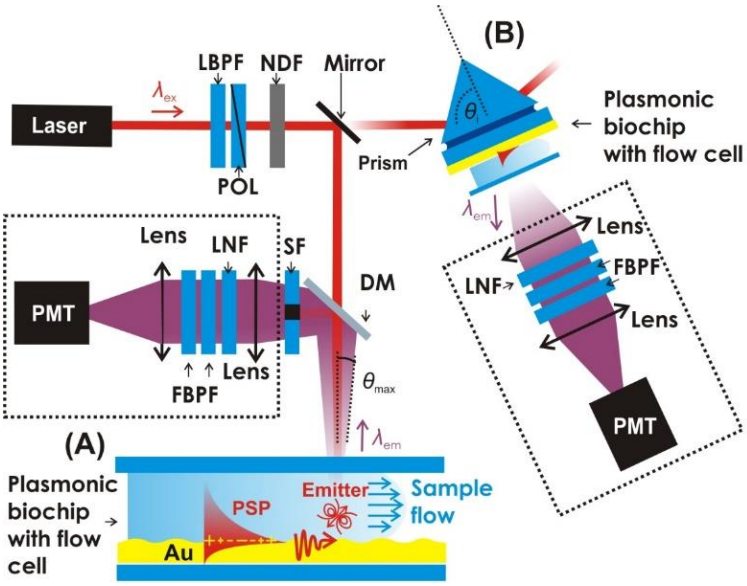

Figure 11: Scheme of used setups: Epifluorescent A) vs. TIRF B) configuration.

4.1.1. Sensor chip preparation

A master crossed grating was prepared by laser interference lithography (LIL). Multiple copies of the master were made using UV nanoimprint lithography (see section 3.2.2). A working stamp was prepared from PDMS elastomer that was cured in contact with the master structure (for 3 days at room temperature) and then detached. A BK7 glass substrate was cut to 20 x 20 mm and cleaned by sequential sonication in 1% Hellmanex in aqueous solution, water, and ethanol. Then, UV curable resin Amonil MMS 10 was spin-coated onto the glass substrate at 3000 rpm for 120 s to form a layer with a thickness of 110 ± 7 nm. Afterwards, the prepared PDMS working stamp with the inverse grating structure was placed onto the Amonil resin and exposed to UV light at λ=365 nm (irritation dose 10 J/cm^2). The PDMS working stamp was detached leaving a copy of master relief grating structure. Each stamp was then used for the preparation of about 8 samples. The samples prepared comprised of an area with the grating structure and a flat area for reference measurements.

The prepared grating structures for EPF measurements were immediately coated with a layer of 4 nm chromium and 100 nm gold by vacuum thermal

evaporation (see section 3.2.2.) utilizing a high vacuum lower than 10^{-6} mBar. For the TIRF measurements, planar cleaned glass substrates were coated with 2 nm of chromium and 45 nm of gold by using the same method.

The corrugation profile of the crossed grating surface was described by using Cartesian coordinates (x and y axis are in the plane of the substrate) as the function $h(x,y)=a(\sin[(2\pi/\Lambda)x] + \sin[(2\pi/\Lambda)y]) + ß(\sin[(2\pi/\Lambda)x] + \sin[(2\pi/\Lambda)y])2$, where Λ is the period and a and β are modulation amplitudes. The parameters of the crossed grating profile used further on are Λ=434 nm, a=4 nm and β=2.5 nm, as determined by atomic force microscopy (AFM) as seen in fig. 12.

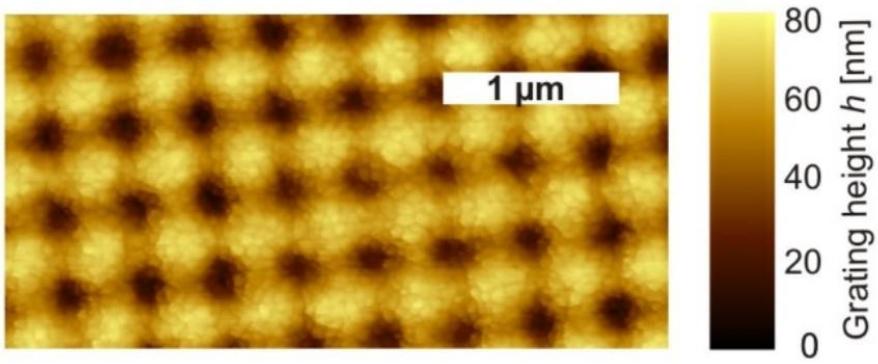

Figure 12: AFM image of gold grating used for the plasmonic amplification in EPF geometry readout.

Directly after the evaporation process, the gold surface of the prepared sensor chip was immersed in a 1 mM solution of PEG and COOH-dithiols dissolved in ethanol at 1:9 ratio and incubated overnight in order to form a SAM. Following that, the surface was thoroughly rinsed with ethanol, dried with a stream of nitrogen, and stored under argon atmosphere until further use. Prior to the experiment, the sensor chip was mounted to the EPF or TIRF optical setup and a flow cell was clamped on top. The sensor chip surface was modified *in situ* with an IL-6 antibody through using amine coupling. In order to activate carboxy-terminal groups on the thiol SAM, the surface was incubated in

an aqueous solution with 21 mg/mL NHS and 75 mg/mL EDC for 15 minutes. Then the surface was rinsed with ACT buffer and a solution with anti-human IL-6 capture antibody dissolved in ACT (pH=4) at a concentration of 50 μg/mL was flowed over the surface. SPR was used for the monitoring of antibody binding and the saturation of reaction was observed after 20 minutes. Finally, unreacted active ester groups were passivated by 1M ethanolamine (pH 8.5) for 20 minutes.

4.1.2. IL-6 sandwich immunoassay

All assay experiments were performed in PBS working buffer with 0.05 % Tween 20 and 1 mg/mL albumin fraction V. Series of samples were prepared by spiking the working buffer with IL-6 at concentrations 1 pg/mL – 100 ng/mL. In addition, standard serum samples were diluted with working buffer at 1:10 ratio. Prior to each assay (shown in fig. 13) the sensor surface was rinsed with working buffer for 5 min in order to establish a baseline in the sensor response (*F)*. Then, the sample to be analyzed was flowed through the sensor for 15 min, followed by 5 min rinsing with working buffer. Afterwards, 1 μg/mL biotin-labelled detection antibody against IL-6 was flowed for 10 minutes. After a 5 min rinsing with working buffer, Alexa Fluor 647 - labelled streptavidin dissolved at 2 μg/mL was flowed and the difference in the sensor signal, ΔF, before and after the assay was determined after additional 5 min rinsing. All samples and reagents were flowed over the sensor at a flow rate of 15 μL/min and the volume of the flow cell was several microlitres.

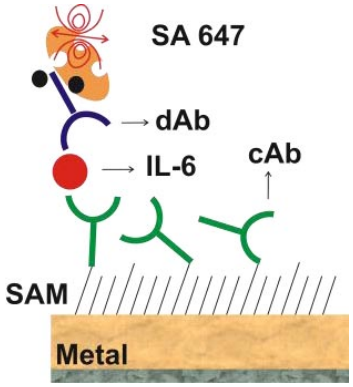

Figure 13: Schematic of the IL-6 detection (cAb-capture antibody, dAB-detection antibody, SA 647 –Streptavidin, fluorescent-labelled).

4.1.3. Comparison of plasmonically amplified EPF and TIRF signal

In order to evaluate the strength of plasmonic amplification for EPF and TIRF readout a series of assays was performed on structured and reference flat gold coated sensor chips. Fig. 14 shows typical fluorescence signal of the kinetics measured upon sequential analysis of samples that were spiked with increasing concentrations of IL-6.

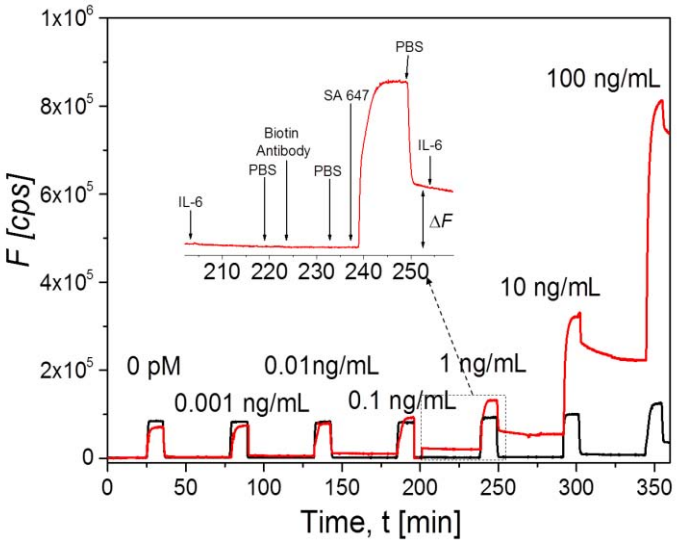

Figure 14: Sensogram showing kinetics on the EPF configuration on grating (red) and plane gold structures (black), including a close-up of one cycle indicating different assay steps.

The data presented are for EPF readout on a flat gold surface (where no plasmonic amplification occurs) and a grating gold surface (where plasmonic amplification occurs). They reveal that crossed grating allowed for the enhancement of fluorescence signal by a factor of about 30 with respect to that measured on reference flat surface.

Sequential series of samples with IL-6 concentrations of 0, 0.001, 0.01, 0.1, 1, 10, 100 ng/mL (equivalent to 0, 0.042, 0.42, 4.2, 42, 4.2×10^2 and 4.2×10^3 pM, respectively) is shown. As explained above, each detection cycle consists of the flowing of the analyte, binding of detection antibody with biotin tags (dAb) and streptavidin carrying Alexa Fluor 647 labels (SA 647). The fluorescence signal F abruptly increases after the injecting of labelled streptavidin due to the excitation of fluorophores in the bulk solution. After the rinsing, this signal drops down to a level that is higher than that of prior to injecting and originates from streptavidin that specifically bound to the detection antibody dAb with a biotin tag. The sensor response ΔF is defined as the difference between fluorescence signal F before injecting the streptavidin and after 5 minutes rinsing with buffer as indicated in the inset graph in fig. 14.

Fig. 15 presents calibration curves for EPF and TIRF readout geometries and the indicated standard deviation obtained from triplicate measurements. From these curves, the limit of detection (LOD) was defined as an intersection of fitted calibration curve (by a sigmoidal function) with the background signal measured for the sample without IL-6 (ΔF_0) plus 3 times standard deviation of the noise signal. It is worth mentioning that ΔF_0 originates from the nonspecific sorption of dAb and SA molecules to the surface. For both plasmonically amplified assay with EPF and TIRF readout, LOD lower than 10 pg/mL was achieved. For reference plane gold samples and EPF geometry, determining the LOD was not possible as the standard deviation was too high.

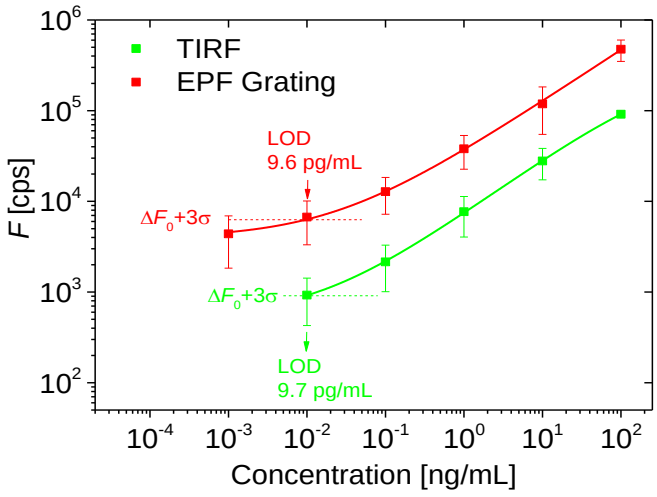

Figure 15: Comparison of sensor response to the assay. Fitting was done using sigmoidal fit, LODs are indicated in dashed horizontal lines.

Lastly, the ability of the sensor to detect IL-6 in real samples is demonstrated by using standard serum samples with analyte concentrations of 8.37, 130.99 and 437.15 pg/mL. In order to suppress the matrix effect, these standards were diluted 1:10 with PBST. The assay was performed identically as described above. Again, the EPF sensor with the crossed grating chip which was functionalized with antibody against IL-6 and additionally, antibody against p53 protein was used as a negative control. The obtained results in fig.16 show that the specific response to the serum standards (on a surface with IL-6 antibodies) is substantially lower than to those in a model assay, presented in fig. 15. This can be ascribed to the diluting of serum samples with buffer. However, when comparing the specific response for anti-IL-6 functionalized chips with a control experiment, all investigated concentrations can be discriminated.

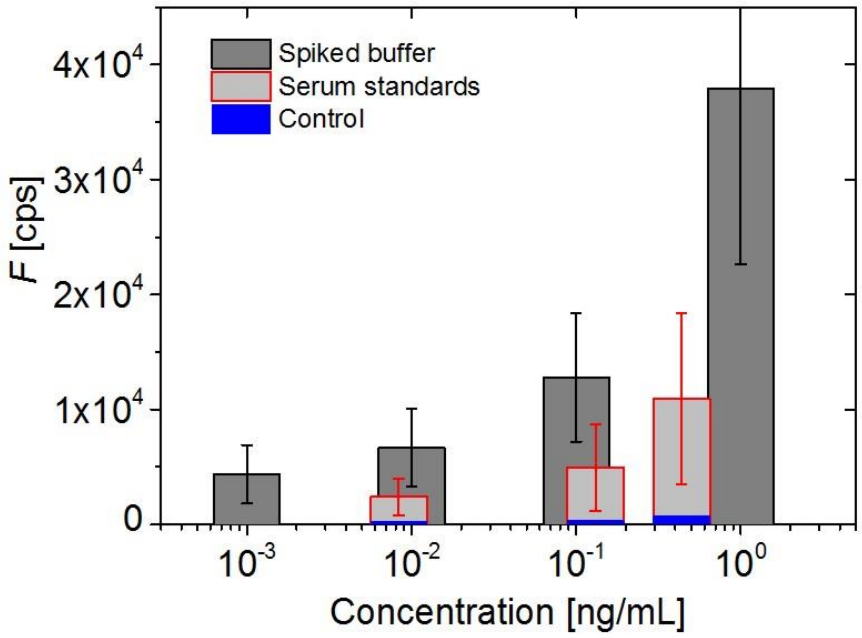

Figure 16: Comparison of the response from EPF sensor with plasmonic grating sensor chip to serum standard samples with IL-6 (diluted 1:10). Black bars represent the calibration curve obtained from spiked buffer samples, red bars show the response to diluted standards on chips carrying anti-IL-6 antibodies and blue bars show the control experiment on anti-p53 antibodies.

4.1.4. Summary

In summary, the experiments reveal that EPF and TIRF configurations perform similarly when applied for readout of fluorescence assays with plasmonic amplification. The plasmonic amplification in EPF shows a higher enhancement of detected fluorescence intensity (a factor of ~13 for the grating surface) while the TIRF geometry that is implemented by Kretschmann configuration enhances the signal strength ~ 4 fold (when compared to EPF readout on a flat substrate). However, in the TIRF geometry the weaker enhancement was compensated by substantially decreased background and the limit of detection < 10 pg/mL was achieved for both platforms. In addition, the

possible discrimination of analyte concentrations < 10 pg/mL in serum was demonstrated.

4.2. Detection of anti-HBs in Clinical Samples

An overview of the experiment principle is depicted in fig. 17.

Serum sample analysis was done using a 4-channel SPR biosensor system (see fig. 17 a and section 3.2.1). The wavelength was tuned to around λ_{res}=800 nm through adjusting the angle of incidence of the collimated polychromatic beam. Sample and reagents were flowed at a flow rate of 15 µl/min into the four chambers (each 1 µl volume), using a peristaltic pump.

Saliva samples were measured using combined angular interrogation of SPR and SPFS (see fig.17 b. and section 3.2.1).

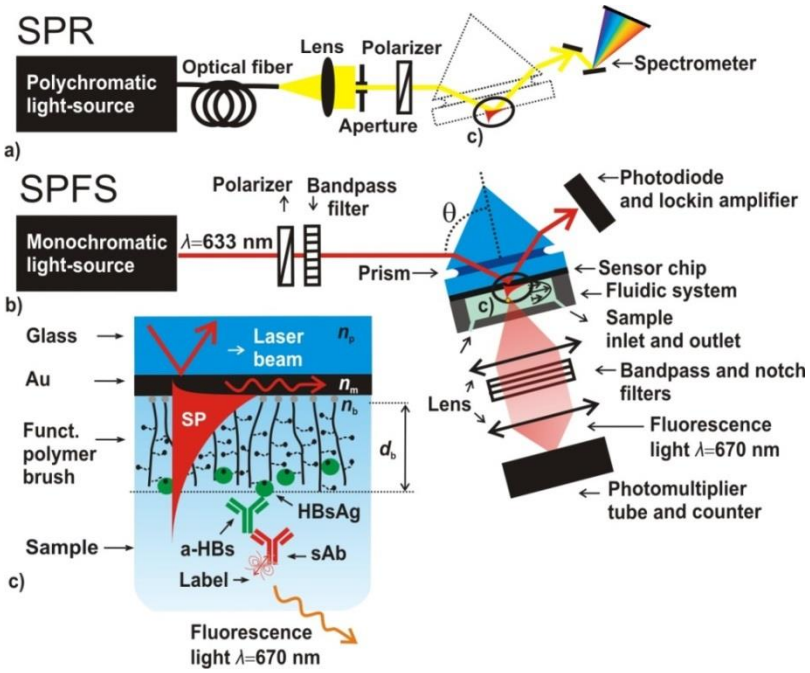

Figure 17: Scheme of the 2 different approaches for detection: a) SPR and b) SPFS and of the surface architecture and c) assay design.

4.2.1. Preparation of the surface

Sensor chips used in these experiments were made from glass substrates coated with 3 nm titanium and 50 nm gold layers (by vacuum evaporation done

at Institute of Photonics and Electronics in Prague). On the gold surface, a SAM with ω-mercaptoundecyl bromoisobutyrate was formed for the subsequent synthesis of the poly(HPMA-co-CBMAA) brush using SI-ATRP (surface initiated-atom transfer radical polymerization). The brush was composed of about 89 % of HPMA and 11 % of CMBAA monomer units. As the BRE for the anti-HBs, HBsAg was immobilized on the surface using amine coupling with EDC/NHS (see section 2.5.4) to the carboxylic groups of CBMAA. The sensor with brush coating was incubated in EDC and NHS dissolved in deioinized water at concentration of 0.2 and 0.05 M, respectively. The incubation time was 15 min. The HBsAg was diluted to 25 μg/mL in HEPES buffer and flowed over the activated brush until a saturation in the binding occurred which was after around 10 min. Afterwards, the sensor surface was washed with PBS in order to hydrolyse unreacted ester groups for 90 min.

Fig. 18 shows an SPR sensogram measured upon the whole immobilization procedure performed. The surface mass density of immobilized HBsAg could be tuned depending on the time of immobilization, and reached a plateau at around 10 minutes, with calculated antigen coverage of 498.6 ng/cm^2.

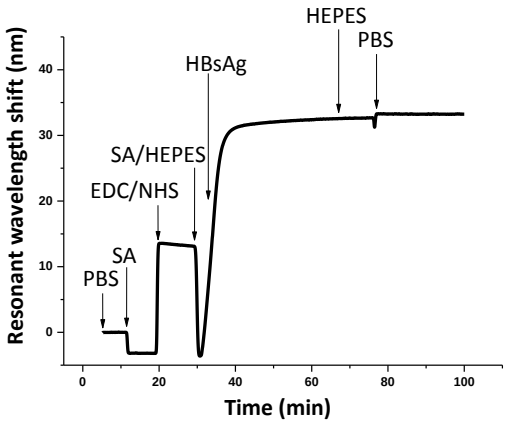

Figure 18: SPR sensogram of the immobilization procedure onto poly(HPMA-co-CBMAA) brushes activated via EDC/NHS. The arrows indicate change of solutions (PBS - phosphate buffered saline buffer, pH 7.4; SA - sodium acetate buffer, pH 5;

HEPES - HEPES buffer, pH 7.5; 0.2M EDC and 0.05M NHS; HBsAg 25 µg/ml in PBS).

4.2.2. Fouling resistance of poly(HPMA-co-CBMAA)brush

In the used brush with a thickness of about 30 nm, the CBMAA monomer provides means for the immobilization of the HBsAg and the HPMA monomer was chosen for anti-fouling properties of the surface. This poly[(N-(2-hydroxypropyl) methacrylamide)-co-(carboxybetaine methacrylamide)] surface architecture was designed to minimize non-specific adsorption from complex media such as serum and saliva. In order to examine these characteristics of the prepared brush, the following SPR measurements were carried out.

The data in fig. 19 below show that when using undiluted saliva and serum, the signal, after rinsing with buffer, is going back to the baseline, thus demonstrating no measureable protein accumulation on the surface and hence effective anti-fouling.

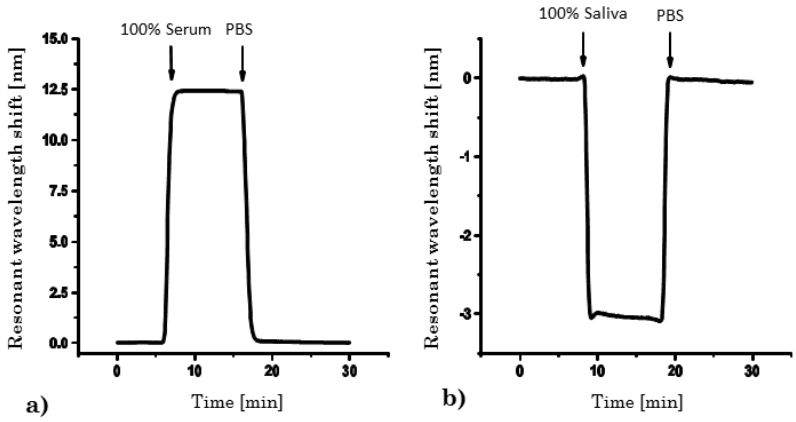

Figure 19: SPR observation of unspecific adsorption from undiluted serum and saliva on polymer brush before HBsAg immobilization.

Additionally, experiments showed that the anti-fouling properties were retained, even after the modification with a ligand. This can be seen in fig. 20, even after immobilization of HBsAg, no measurable fouling from 10 fold diluted serum was observed on the sensing surface, demonstrating high anti-fouling properties of the brush.

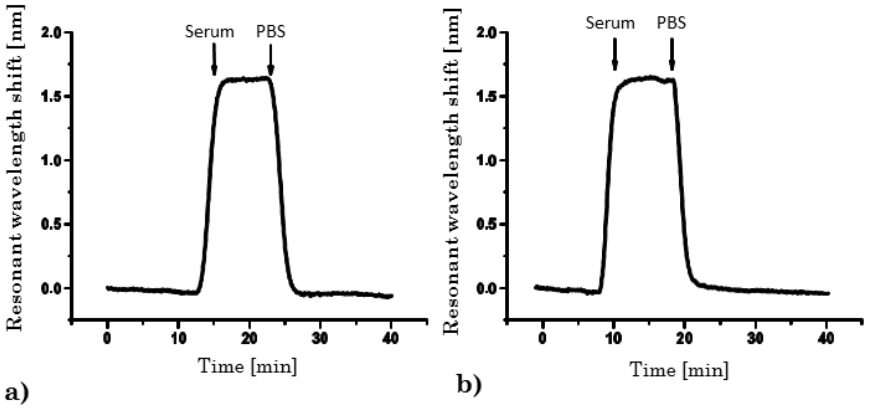

Figure 20: SPR observation of non-specifically bound biomolecules from 10% serum at the polymer brush a) after synthesis and b) after it was modified by HBsAg

For experiments in fig. 19 and 20, serum and saliva without anti-HBs was used, from an unvaccinated person with no prior infection (confirmed by independent laboratory).

4.2.3. Analyzed samples

Eight clinical serum and saliva samples were collected from healthy donors. The serum samples were tested for the presence of anti-HBs by ELISA in certified laboratory as summarized in Table 1. Three of them (sample 4,6,8) were characterized as negative as they were obtained from unvaccinated individuals, three of them (sample 2,5,7) were positive (68-645 mIU/mL) and two (sample 1,3) were highly positive (<1000 mIU/mL).

Table 1: Serum samples and their concentrations of anti-HBs tested by an independent laboratory.

Samples	Serum 1	Serum 2	Serum 3	Serum 4	Serum 5	Serum 6	Serum 7	Serum 8
mIU/ml	>1000	68	> 1000	0	162	0	645	0

4.2.4. SPR analysis of serum samples

Using a regular SPR sensor, the affinity binding of antibodies against HBsAg from the serum samples (10-fold diluted by PBS) was measured. Each sample was flowed over a sensor chip with antifouling brush and covalently immobilized antigen for 10 min followed by a 5 min rinsing with PBS. The response to affinity binding of human anti-HBs was evaluated as a difference in the SPR wavelength before sample injection and after 5 min rinsing with PBS. Afterwards, a secondary antibody (anti-human IgG) at a concentration of 2 μg/mL in PBS was flowed over the surface for 10 mins in order to amplify the response.

Examples of measured sensograms for serum samples are presented in fig. 21. In each experiment, an abrupt change in SPR wavelength is observed after a serum sample is injected (t=10 min) and after the rinsing with buffer (t=20 min). The reason is the bulk refractive index change associated with the high protein concentration in serum samples. After washing with PBS, the response equilibrates at a level that is above the original baseline for positive samples showing affinity binding of the anti-HBs to the surface.

In order to confirm the presence of affinity captured antibodies against these HBsAg, response to secondary anti-human IgG was measured. The results obtained using a sandwich assay were consistent with those from the direct detection assay.

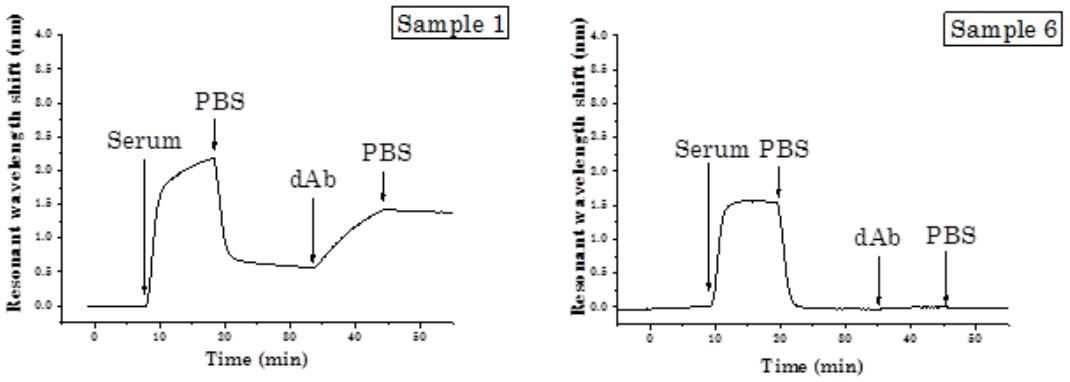

Figure 21: Examples of SPR analysis of serum samples with direct and indirect sandwich assay for a sample which is highly positive (sample 1) and one which is negative (sample 6).

Clearly positive and negative samples can be distinguished, most even without using 2nd AB detection. The sandwich assay confirmed the results from the direct assay, as can be seen in fig. 22.

Furthermore, the sensor response to direct and secondary amplified detection was compared to ELISA results. The summary of these measurements is presented in fig. 22.

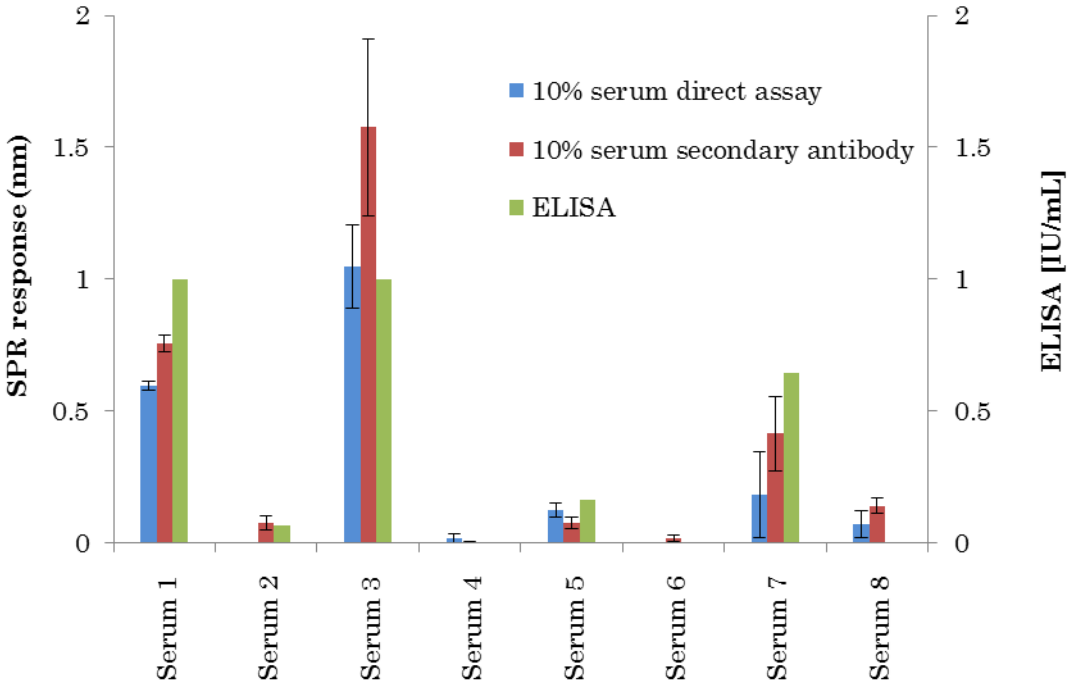

Figure 22: Detection of anti-HBs antibodies in serum samples comparing SPR using a direct assay (blue), sandwich assay (red) and ELISA (green). All samples were measured in triplicate and the error bar represents the standard deviation.

In general, the SPR detection proved its capability of real time analysis of clinical serum samples, with a detection time of only 10 min and 10 µl of sample needed for the direct assay.

4.2.5. SPFS analysis of saliva samples

Even though the SPR platform provided strong signal associated to the binding of anti-HBs present serum, the analysis of saliva samples obtained from the same individual did not show a measurable response. This could be ascribed to the fact that the concentrations of IgG antibodies present in saliva are orders of magnitude below the levels in blood (Engström et al., 1996), as most IgGs in saliva derive from serum through gingival crevicular fluid (Kaufman and Lamster, 2002) (Hofman, 2001).

Therefore, SPFS was employed on identical sensor chips with the same sandwich assay and identical secondary antibody that was labelled with fluorophores. In the fluorescence measurements, as shown in fig. 23, the differences in the fluorescence signal ΔF before and after the secondary antibody binding was assumed as the sensor response.

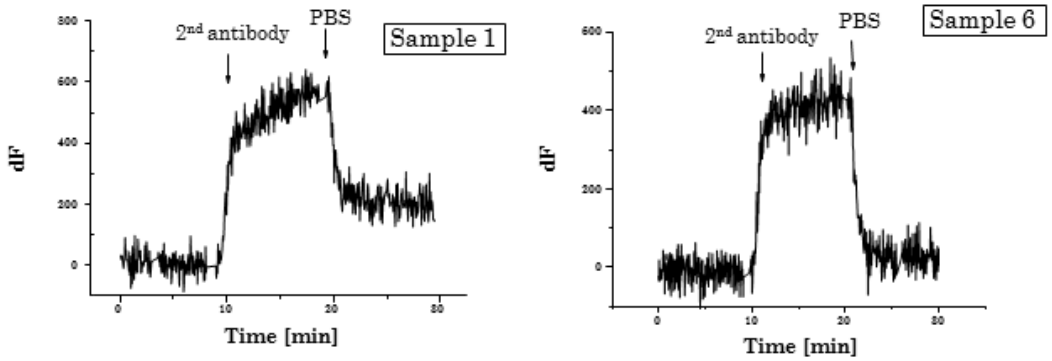

Figure 23: Examples of SPFS analysis in saliva samples with high concentration of anti-HBs (sample 1) and no antibodies (sample 6).

In order to compensate for variations in the alignment, this response was normalized by that of a reference sample measured prior to the saliva analysis on the same chip with the same sensor alignment. Firstly, 10 pM mouse anti-HBs were flowed over the sensor for 10 min and after a 5 min rinsing with PBS 4 µg/mL Alexa Fluor 647 labelled anti-mouse IgG were flowed. The difference in sensor signal, $\Delta F_{cal,}$ was used afterwards to normalize the measured response to human anti-HBs. The whole assay cycle is illustrated in figure 24.

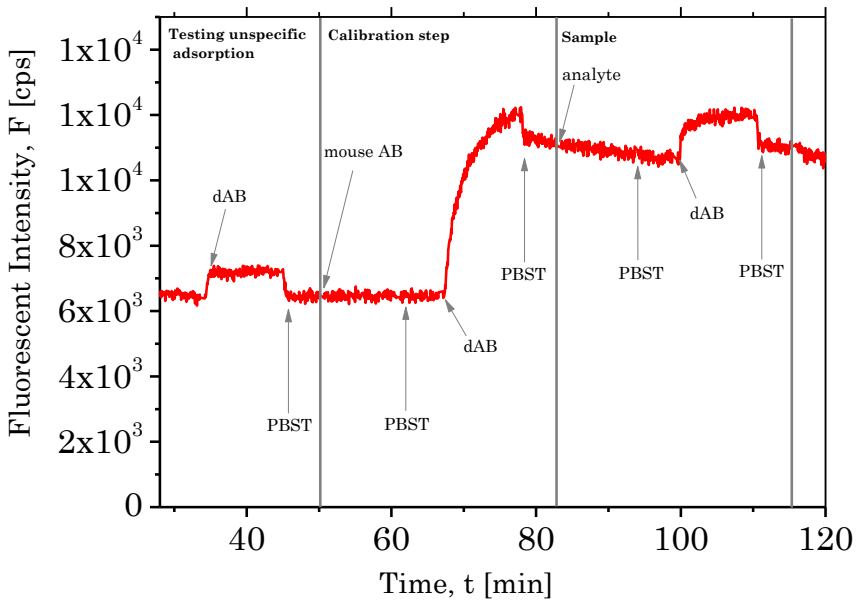

Figure 24: Example of one experiment cycle: here an identical measurement is shown on a SAM surface.

The results for all tested saliva samples are summarized in fig. 25 as the ratio of the saliva signal divided by the calibration step signal.

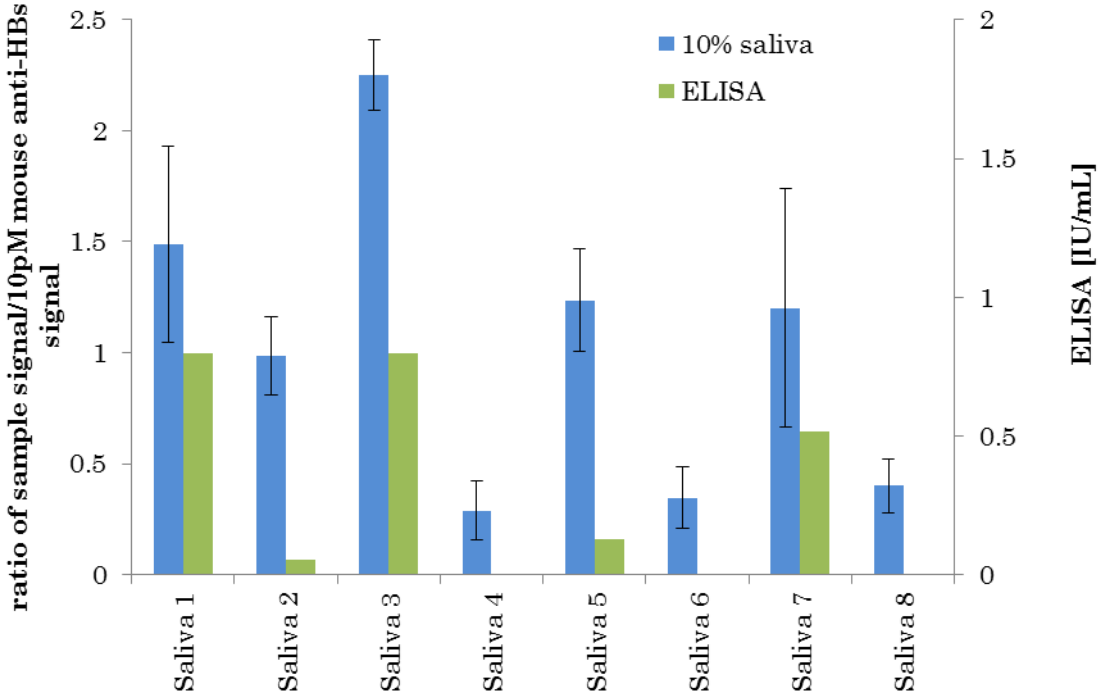

Figure 25: Detection of anti-HBs antibodies in saliva samples comparing SPFS (grey) and ELISA (black) detection. All samples were measured in triplicate and the error bar represents the standard deviation.

The highly positive samples 1 and 3 gave the highest response and were distinguishable from the negative samples 4, 6 and 8.

In addition, even negative samples showed relatively strong response. Therefore, the quantitative evaluation of positive saliva samples was not possible and only a qualitative result can be given. Interestingly, the differences in response between different saliva samples were much lower than that measured in serum. Indeed, this can be attributed to the fact that the concentration of a protein present in serum is not necessarily proportional to that in saliva. The saliva composition varies in individuals as well as in the same individual under different conditions (e.g. light, day time, nutrition, behaviour, medication), with the collection method and the flow rate. Additional

factors like microorganisms and their enzymes or medication can affect the stability of the samples. Therefore the diagnosis in saliva will remain a difficult task (Kaufman and Lamster, 2002).

In order to develop more reliable diagnostic tools for saliva testing, these numerous factors and controlled sample collection have to be taken into account, especially when detecting serum-derived biomarkers. Especially in the assay presented here, there should be a way found to develop more advanced referencing of the response (e.g. measure total IgG concentration).

5. Conclusion

In the course of this thesis, several biosensor concepts that are attractive for rapid detection of trace amounts of biomarkers in bodily fluids were demonstrated. In particular, the thesis concerns new means for amplification of the fluorescence biosensor response and explores new biointerface architectures for eliminating unspecific interactions with the sensor surface and thus enables analysis of complex samples.

The detection of IL-6 in medically relevant concentrations was shown to be possible with the newly developed EPF biosensor platform as well as with the already established TIRF platform, showing similar performances. Therefore this successful implementation of the IL-6 immunoassay showed that the developed nanostructures and EPF readout can possibly be used in combination with commercial fluorescence readers, enabling monitoring of real-time binding events.

The developed biosensor for the detection of anti-HB antibodies using a novel copolymer brush showed an excellent anti-fouling surface while simultaneously being able to be functionalized with proteins. Detection in clinical serum samples could be done in real-time and label-free using a SPR biosensor and results were confirmed using a sandwich assay. Even in saliva samples, a matrix known for high surface fouling, with a very low level of antibodies, a qualitative result could be obtained through detection with SPFS using a sandwich assay. For future applications, the developed brush architecture holds great potential to be employed for a range of analytes, especially in saliva samples, which can be obtained non-invasively.

Generally speaking, the possibility to provide highly sensitive sensor platforms for the detection of biomarkers could greatly impact the rapidly developing field of POCT and potentially translate to a new class of practical

technology. The results and concepts presented here can be of value for the implementation into portable biosensor devices outside centralized laboratory infrastructure.

Publications

1) Bauch, M., **Hageneder, S**., and Dostálek, J. (2014). Plasmonic amplification for bioassays with epi-fluorescence readout. Opt. Express *22*, 32026.

2) **Hageneder, S**., Bauch, M., Dostálek J. (in preparation). Plasmonically amplified fluorescence bioassays – total internal reflection vs. epifluorescence geometry, (2015), in preparation.

3) Riedel, T. Surman, F., **Hageneder, S**., et al. (2015). Detection of antibodies against Hepatitis B in clinical serum and saliva samples, Biosensors and Bioelectronics (2015), in preparation.

4) Geddes, C.D. (2015). Surface plasmon enhanced, coupled and controlled fluorescence. (John Wiley).

References

Anestakis, D., Petanidis, S., Kalyvas, S., Nday, C., Tsave, O., Kioseoglou, E., and Salifoglou, A. (2015). Mechanisms and Applications of Interleukins in Cancer Immunotherapy. Int. J. Mol. Sci. *16*, 1691–1710.

Bauch, M. (2014). New enhancement strategies for plasmon-enhanced fluorescence biosensors. Universitätsbibliothek Mainz.

Bauch, M., Hageneder, S., and Dostalek, J. (2014). Plasmonic amplification for bioassays with epi-fluorescence readout. Opt. Express *22*, 32026.

Biacore (2015). Biacore Life Sciences.

Blaszykowski, C., Sheikh, S., and Thompson, M. (2012). Surface chemistry to minimize fouling from blood-based fluids. Chem. Soc. Rev. *41*, 5599.

Blumberg, B.S. (1977). Australia antigen and the biology of hepatitis B (Nobel Foundation).

Boozer, C., Kim, G., Cong, S., Guan, H., and Londergan, T. (2006). Looking towards label-free biomolecular interaction analysis in a high-throughput format: a review of new surface plasmon resonance technologies. Curr. Opin. Biotechnol. *17*, 400–405.

Brinkley, M. (1992). A brief survey of methods for preparing protein conjugates with dyes, haptens and crosslinking reagents. Bioconjug. Chem. *3*, 2–13.

Busse, S., Scheumann, V., Menges, B., and Mittler, S. (2002). Sensitivity studies for specific binding reactions using the biotin/streptavidin system by evanescent optical methods. Biosens. Bioelectron. *17*, 704–710.

Chambers, J.P., Arulanandam, B.P., Matta, L.L., Weis, A., and Valdes, J.J. (2008). Biosensor recognition elements. Curr. Issues Mol. Biol. *10*, 1–12.

Chen, S., Li, L., Boozer, C.L., and Jiang, S. (2000). Controlled Chemical and Structural Properties of Mixed Self-Assembled Monolayers of Alkanethiols on Au(111). Langmuir *16*, 9287–9293.

Chen, S., Yu, F., Yu, Q., He, Y., and Jiang, S. (2006). Strong Resistance of a Thin Crystalline Layer of Balanced Charged Groups to Protein Adsorption. Langmuir *22*, 8186–8191.

REFERENCES

Cullen, D.C., Brown, R.G.W., and Lowe, C.R. (1987). Detection of immuno-complex formation via surface plasmon resonance on gold-coated diffraction gratings. Biosensors *3*, 211–225.

Danai, P., and Martin, G.S. (2005). Epidemiology of sepsis: recent advances. Curr. Infect. Dis. Rep. *7*, 329–334.

Dostálek, J., and Homola, J. (2006). SPR Biosensors for Environmental Monitoring. In Surface Plasmon Resonance Based Sensors, J. Homola, ed. (Berlin, Heidelberg: Springer Berlin Heidelberg), pp. 191–206.

Dostálek, J., and Knoll, W. (2008). Biosensors based on surface plasmon-enhanced fluorescence spectroscopy (Review). Biointerphases *3*, FD12.

Dostálek, J., Ladd, J., Jiang, S., and Homola, J. (2006). SPR Biosensors for Detection of Biological and Chemical Analytes. In Surface Plasmon Resonance Based Sensors, J. Homola, ed. (Springer Berlin Heidelberg), pp. 177–190.

Drexhage, K.H. (1970). Influence of a dielectric interface on fluorescence decay time. J. Lumin. *1*, 693–701.

Ekgasit, S., Thammacharoen, C., Yu, F., and Knoll, W. (2005). Influence of the Metal Film Thickness on the Sensitivity of Surface Plasmon Resonance Biosensors. Appl. Spectrosc. *59*, 661–667.

Engström, P.E., Norhagen, G., Osipova, L., Helal, A., Wiebe, V., Brusco, A., Carbonara, A.O., Lefranc, G., and Lefranc, M.P. (1996). Salivary IgG subclasses in individuals with and without homozygous IGHG gene deletions. Immunology *89*, 178–182.

Engvall, E., and Perlmann, P. (1971). Enzyme-linked immunosorbent assay (ELISA) quantitative assay of immunoglobulin G. Immunochemistry *8*, 871–874.

Fischer, C.P. (2006). Interleukin-6 in acute exercise and training: what is the biological relevance. Exerc Immunol Rev *12*, 41.

Foran, E., Garrity-Park, M.M., Mureau, C., Newell, J., Smyrk, T.C., Limburg, P.J., and Egan, L.J. (2010). Upregulation of DNA Methyltransferase-Mediated Gene Silencing, Anchorage-Independent Growth, and Migration of Colon Cancer Cells by Interleukin-6. Mol. Cancer Res. *8*, 471–481.

Gaebel, W., and Zielasek, J. (2008). Die Rolle von Biomarkern aus der Sicht der wissenschaftlichen Fachgesellschaften. In Biomarker:, (Schattauer),.

Gitlin, N. (1997). Hepatitis B: diagnosis, prevention, and treatment. Clin. Chem. *43*, 1500–1506.

Gitlin, G., Bayer, E.A., and Wilchek, M. (1990). Studies on the biotin-binding sites of avidin and streptavidin. Tyrosine residues are involved in the binding site. Biochem. J. *269*, 527–530.

Great Britain Department of Health, and Joint Committee on Vaccination and Immunisation (2006). Chapter 18 Hepatitis B Immunisation Against Infectious Disease 2006. In Immunisation against Infectious Disease. 2006 2006, (Norwich: TSO),.

Gryczynski, I., Malicka, J., Gryczynski, Z., and Lakowicz, J.R. (2004). Radiative decay engineering 4. Experimental studies of surface plasmon-coupled directional emission. Anal. Biochem. *324*, 170–182.

Harbarth, S., Holeckova, K., Froidevaux, C., Pittet, D., Ricou, B., Grau, G.E., Vadas, L., and Pugin, J. (2001). Diagnostic value of procalcitonin, interleukin-6, and interleukin-8 in critically ill patients admitted with suspected sepsis. Am. J. Respir. Crit. Care Med. *164*, 396–402.

Herrwerth, S., Eck, W., Reinhardt, S., and Grunze, M. (2003). Factors that Determine the Protein Resistance of Oligoether Self-Assembled Monolayers − Internal Hydrophilicity, Terminal Hydrophilicity, and Lateral Packing Density. J. Am. Chem. Soc. *125*, 9359–9366.

Hofman, L.F. (2001). Human saliva as a diagnostic specimen. J. Nutr. *131*, 1621S – 1625S.

Homola, J. (2003). Present and future of surface plasmon resonance biosensors. Anal. Bioanal. Chem. *377*, 528–539.

Homola, J., Yee, S.S., and Gauglitz, G. (1999). Surface plasmon resonance sensors: review. Sens. Actuators B Chem. *54*, 3–15.

Homola, J., Vaisocherová, H., Dostálek, J., and Piliarik, M. (2005). Multi-analyte surface plasmon resonance biosensing. Methods *37*, 26–36.

Huang, C.-J., Dostalek, J., Sessitsch, A., and Knoll, W. (2011). Long-Range Surface Plasmon-Enhanced Fluorescence Spectroscopy Biosensor for Ultrasensitive Detection of *E. coli* O157:H7. Anal. Chem. *83*, 674–677.

Huzly, D., Schenk, T., Jilg, W., and Neumann-Haefelin, D. (2008). Comparison of Nine Commercially Available Assays for Quantification of Antibody Response to Hepatitis B Virus Surface Antigen. J. Clin. Microbiol. *46*, 1298–1306.

Jawad, I., Lukšić, I., and Rafnsson, S.B. (2012). Assessing available information on the burden of sepsis: global estimates of incidence, prevalence and mortality. J. Glob. Health *2*, 010404.

Jekarl, D.W., Lee, S.-Y., Lee, J., Park, Y.-J., Kim, Y., Park, J.H., Wee, J.H., and Choi, S.P. (2013). Procalcitonin as a diagnostic marker and IL-6 as a prognostic marker for sepsis. Diagn. Microbiol. Infect. Dis. *75*, 342–347.

Jiang, S., and Cao, Z. (2010). Ultralow-Fouling, Functionalizable, and Hydrolyzable Zwitterionic Materials and Their Derivatives for Biological Applications. Adv. Mater. *22*, 920–932.

Jones, S.A. (2005). Directing transition from innate to acquired immunity: defining a role for IL-6. J. Immunol. *175*, 3463–3468.

Kaufman, E., and Lamster, I.B. (2002). The diagnostic applications of saliva—a review. Crit. Rev. Oral Biol. Med. *13*, 197–212.

Knoll, W., Liley, M., Piscevic, D., Spinke, J., and Tarlov, M.J. (1997). Supramolecular architectures for the functionalization of solid surfaces. Adv. Biophys. *34*, 231–251.

Knudsen, L.S., Christensen, I.J., Lottenburger, T., Svendsen, M.N., Nielsen, H.J., Nielsen, L., Hørslev-Petersen, K., Jensen, J.E.B., Kollerup, G., and Johansen, J.S. (2008). Pre-analytical and biological variability in circulating interleukin 6 in healthy subjects and patients with rheumatoid arthritis. Biomarkers *13*, 59–78.

Kost, G.J., Ehrmeyer, S.S., Chernow, B., Winkelman, J.W., Zaloga, G.P., Dellinger, R.P., and Shirey, T. (1999). The laboratory-clinical interface: point-of-care testing. CHEST J. *115*, 1140–1154.

Kresge, N., Simoni, R.D., and Hill, R.L. (2004). The Discovery of Avidin by Esmond E. Snell. J. Biol. Chem. *279*, e5–e5.

Kretschmann, E, and Raether, H. (1968). Radiative Decay of Non Radiative Surface Plasmons Excited by Light. Z.Naturforsch 2135–2136.

Lakowicz, J.R. (2004). Radiative decay engineering 3. Surface plasmon-coupled directional emission. Anal. Biochem. *324*, 153–169.

Lakowicz, J.R. (2005). Radiative decay engineering 5: metal-enhanced fluorescence and plasmon emission. Anal. Biochem. *337*, 171–194.

Lakowicz, J.R. (2006). Principles of fluorescence spectroscopy (New York: Springer).

Lee, Y.-H., and Wong, D.T. (2009). Saliva: an emerging biofluid for early detection of diseases. Am. J. Dent. *22*, 241.

Liebermann, T., and Knoll, W. (2000). Surface-plasmon field-enhanced fluorescence spectroscopy. Colloids Surf. Physicochem. Eng. Asp. *171*, 115–130.

Liedberg, B., Nylander, C., and Lunström, I. (1983). Surface plasmon resonance for gas detection and biosensing. Sens. Actuators *4*, 299–304.

Liley, M. (2002). Optical transducers. In Biomolecular Sensors, (London; New York: Taylor & Francis),.

Löfås, S., and Mcwhirter, A. (2006). The Art of Immobilization for SPR Sensors. In Surface Plasmon Resonance Based Sensors, J. Homola, ed. (Berlin, Heidelberg: Springer Berlin Heidelberg), pp. 117–151.

Long, F., Zhu, A., and Shi, H. (2013). Recent Advances in Optical Biosensors for Environmental Monitoring and Early Warning. Sensors *13*, 13928–13948.

Love, J.C., Estroff, L.A., Kriebel, J.K., Nuzzo, R.G., and Whitesides, G.M. (2005). Self-Assembled Monolayers of Thiolates on Metals as a Form of Nanotechnology. Chem. Rev. *105*, 1103–1170.

Lowe, C.R. (1985). An introduction to the concepts and technology of biosensors. Biosensors *1*, 3–16.

Mahoney, F.J. (1999). Update on diagnosis, management, and prevention of hepatitis B virus infection. Clin. Microbiol. Rev. *12*, 351–366.

Mascini, M., and Tombelli, S. (2008). Biosensors for biomarkers in medical diagnostics. Biomarkers *13*, 637–657.

Milena Biotec (2015). Milenia Biotec GmbH | Milenia® QuickLine IL-6.

Narain, R., and Sunasee, R. (2014). Covalent and Noncovalent Bioconjugation Strategies. In Chemistry of Bioconjugates: Synthesis, Characterization, and Biomedical Applications, R. Narain, ed.

Neumann, T., Johansson, M.-L., Kambhampati, D., and Knoll, W. (2002). Surface–Plasmon Fluorescence Spectroscopy. Adv. Funct. Mater. *12*, 575–586.

Otto, A. (1968). Excitation of nonradiative surface plasma waves in silver by the method of frustrated total reflection. Z. Für Phys. *216*, 398–410.

Poorolajal, J., Mahmoodi, M., Majdzadeh, R., Nasseri-Moghaddam, S., Haghdoost, A., and Fotouhi, A. (2010). Long-term protection provided by hepatitis B vaccine and need for booster dose: A meta-analysis. Vaccine *28*, 623–631.

Roche GmbH (2015). Elecsys® IL-6 - Diagnostics - Roche in Deutschland.

Rodriguez-Emmenegger, C., Schmidt, B.V.K.J., Sedlakova, Z., Šubr, V., Alles, A.B., Brynda, E., and Barner-Kowollik, C. (2011a). Low Temperature Aqueous Living/Controlled (RAFT) Polymerization of Carboxybetaine Methacrylamide up to High Molecular Weights. Macromol. Rapid Commun. *32*, 958–965.

Rodriguez-Emmenegger, C., Brynda, E., Riedel, T., Houska, M., Šubr, V., Alles, A.B., Hasan, E., Gautrot, J.E., and Huck, W.T.S. (2011b). Polymer Brushes Showing Non-Fouling in Blood Plasma Challenge the Currently Accepted Design of Protein Resistant Surfaces. Macromol. Rapid Commun. *32*, 952–957.

Rodriguez-Emmenegger, C., Houska, M., Alles, A.B., and Brynda, E. (2012). Surfaces Resistant to Fouling from Biological Fluids: Towards Bioactive Surfaces for Real Applications. Macromol. Biosci. *12*, 1413–1422.

Schreiber, F. (2000). Structure and growth of self-assembling monolayers. Prog. Surf. Sci. *65*, 151–257.

Spinke, J., Liley, M., Guder, H.J., Angermaier, L., and Knoll, W. (1993). Molecular recognition at self-assembled monolayers: the construction of multicomponent multilayers. Langmuir *9*, 1821–1825.

Stratis-Cullum, D., and Sumner, J. (2010). Biosenors and Bioelectronics. In Bio-Inspired Innovation and National Security, R.E. Armstrong, ed. (Washington, D.C. : Published for the Center for Technology and National Security Policy by National Defense University Press :),.

Subramanian, A., Irudayaraj, J., and Ryan, T. (2006). Mono and dithiol surfaces on surface plasmon resonance biosensors for detection of Staphylococcus aureus. Sens. Actuators B Chem. *114*, 192–198.

Szunerits, S., Castel, X., and Boukherroub, R. (2008). Surface Plasmon Resonance Investigation of Silver and Gold Films Coated with Thin Indium Tin Oxide Layers: Influence on Stability and Sensitivity. J. Phys. Chem. C *112*, 15813–15817.

Thermo Fisher Scientific Inc. (2009). Avidin-Biotin Handbook.

Toma, K., Toma, M., Bauch, M., Hageneder, S., and Dostalek, J. (2015). Fluorescence biosensors utilizing grating-assisted plasmonic amplification. In Surface Plasmon Enhanced, Coupled and Controlled Fluorescence, C.D. Geddes, ed.

Ulbrich, K., Šubr, V., Strohalm, J., Plocova, D., Jelınková, M., and Říhová, B. (2000). Polymeric drugs based on conjugates of synthetic and natural macromolecules: I. Synthesis and physico-chemical characterisation. J. Controlled Release *64*, 63–79.

Van Weemen, B.K., and Schuurs, A. (1971). Immunoassay using antigen—enzyme conjugates. FEBS Lett. *15*, 232–236.

Vericat, C., Vela, M.E., Benitez, G., Carro, P., and Salvarezza, R.C. (2010). Self-assembled monolayers of thiols and dithiols on gold: new challenges for a well-known system. Chem. Soc. Rev. *39*, 1805.

Weber, W.H., and Eagen, C.F. (1979). Energy transfer from an excited dye molecule to the surface plasmons of an adjacent metal. Opt. Lett. *4*, 236.

Wilchek, M., and Bayer, E.A. (1998). Avidin-biotin immobilzation systems. In Immobilized Biomolecules in Analysis: A Practical Approach, T. Cass, and F.S. Ligler, eds. (Oxford: Oxford Univ. Press),.

Wild, D. (2013). The immunoassay handbook: theory and applications of ligand binding, ELISA and related techniques (Newnes).

van Wolferen, H., and Abelmann, L. (2011). Laser Interference Lithography. In Lithography Principles, Processes, and Materials, T.C. Hennessy, ed. (New York: Nova Science),.

Yalow, R.S., and Berson, S.A. (1959). Assay of Plasma Insulin in Human Subjects by Immunological Methods. Nature *184*, 1648–1649.

Yu, F., Persson, B., Löfås, S., and Knoll, W. (2004). Attomolar Sensitivity in Bioassays Based on Surface Plasmon Fluorescence Spectroscopy. J. Am. Chem. Soc. *126*, 8902–8903.